TÜBİTAK

Turkish Journal of Botany

http://journals.tubitak.gov.tr/botany/

Research Article

Turk J Bot
(2022) 46: 435-458
© TÜBİTAK
doi:10.55730/1300-008X.2721

Modulation of physiological plasticity through structural and functional modifications in *Stipagrostis plumosa* L. for adaptability to hyperarid environments

Safura BIBI[1]*, Muhammad Sajid Aqeel AHMAD[1], Mansoor HAMEED[1], Ambreen Khadija ALVI[2]
[1]Department of Botany, University of Agriculture, Faisalabad, Pakistan
[2]Department of Botany, Government College Women University, Faisalabad, Pakistan

Received: 14.11.2021 • **Accepted/Published Online:** 28.06.2022 • **Final Version:** 19.09.2022

Abstract: The role of morpho-physiological attributes along with the antioxidant potential of *Stipagrostis plumosa* L. populations collected from arid regions in adaptability to aridity was evaluated. Root to shoot length, chlorophyll, carotenoids, and organic osmolytes (total free amino acids, total soluble proteins, glycinebetaine, and proline) increased with more activities of antioxidant enzymes (APX, CAT, POD, and SOD). Root and shoot fresh:dry weight ratio and leaf area decreased with increasing dryness ratio (D: 8.40–30.49) and decreasing precipitation (519 mm to 143 mm). Hyperarid populations [Noorpur Thal - NpT (D: 10.90; P: 400 mm) and Cholistan - Cho (D:30.49; P: 143 mm)] relied on reduced leaf area and plant biomass, longer roots, more activities of antioxidant enzymes with higher accumulation of organic osmolytes, and better compartmentation of ions in root and shoot. Root and leaf epidermal thicknesses, epidermal cell area, the proportion of cortical parenchyma, metaxylem cell area, abaxial stomatal density and area reduced significantly while stem epidermis thickness, cortical cell area, and metaxylem cell area increased in relatively less arid populations [Neela Wahn-NeW (D: 8.40; P: 519 mm) and Kallar Kahar-KKr (D: 8.99; P: 485 mm)]. In conclusion, survival of *S. plumosa* under water deficit was directly linked to the plasticity in morpho-physiological and anatomical traits such as epidermal hairs, thick leaves, intense sclerification in roots epidermis, cortex and endodermis, and vascular bundle. These traits not only accounted for the movement of water and solutes but also help conserve water and provided mechanical strength for survival in hyperarid environments.

Key words: Osmolytes, antioxidants, root, anatomy, adaptations, hyperarid environments

1. Introduction

Changing climatic conditions around the world indicate that many areas of the globe are at risk of aridity. Water deficit affects all living organisms, especially plants which do not have locomotive structures that allow them to move elsewhere when water and food become limited (Eziz et al., 2017). Changes in rainfall pattern and temperature had substantially altered water availability in soil. This puts many restrictions on plant growth and survival of vegetation already thriving for survival in extreme water deficit environments of desert habitats (Ivanova et al., 2018).

Arid areas are the regions with irregular and low rainfall patterns leading to deficiency of water. There are many classifications used to group arid regions. For example, Hare (1985) classified arid regions by Budyko-Lettau dryness ratio (D) as an aridity index. This ratio was based on annual net radiation energy received at the earth surface to the heat energy needed for evaporation. This classification groups arid regions as normal (D < 2.3), semidesert (D > 2.3), desert (D ≥ 3.4) and extreme desert (D ≥ 10; UNESCO 1979). According to another classification by UNESCO, hyperarid areas are characterized by extremely low (30–50 mm per annum) and irregular rainfall that supports seasonal vegetation while annual rainfall of 80–350 mm supports scattered vegetation in arid areas. Semiarid areas are characterized by mean annual rainfall between 300–900 mm with perennial grass species. A dryness (D) ratio of greater than 2 is reported for the hyperarid zone and greater than 10 is for desert while semiarid and arid regions lie in between (UNEP, 1997; Huang et al., 2016).

Various mechanisms allow plants to survive in arid conditions by maximizing water uptake using deep, dense root systems. This minimizes water loss by closing stomata, reducing leaf area and osmotic adjustment in cells as well as through other processes for maintaining physiological activities in extended periods of arid conditions (Zhou et al., 2021). Stunted growth and plant mortality is observed when water stress becomes too severe or persists over long time periods (Kidd et al., 2018). Root length and density increase with increasing soil moisture deficit for deeper

* Correspondence: safurabotany@gmail.com

penetration to extract water from deeper layers (Kidd et al., 2021). In a past study, photosynthetic pigments (chlorophyll and carotenoids) decreased in *L. scindicus* with increasing water and salt stress (Bahar et al., 2018).

Plants from arid regions tolerate water deficit by modifying osmoregulatory mechanisms along with several morphological changes. These plants accumulate various solutes such as inorganic ions, organic osmolytes, and antioxidative enzymes. They play a role in osmoprotection and ROS, the scavenging reactive oxygen species (Kapoor et al., 2020). Free amino acids, proline, and sugars are the organic osmolytes that show a significantly variable accumulation under water stress. These solutes have a protective effect on enzymes in the presence of high electrolytes. More concentration of these solutes in the cytoplasm plays a protective effect on enzymes (Cuizhi et al., 2021). These plants growing in water deficit environments also exhibit certain anatomical adaptations such as sclerified leaves, roots epidermis and endodermis, leaf pubescence and root hairs (Susetyarini et al., 2020).

Stipagrostis plumosa is widely distributed in arid regions of Africa, Middle East, India and Pakistan. It is densely tufted perennials with knotty rhizomatous base, narrow leaf blade, chlorophyll-bearing culms as the main photosynthetic organs with distinguishable plumose awns (Majeed et al., 2022). Due to wider distribution in hyperarid areas because of drought-resistance, it is of particular importance to grazing animals in both fresh and dried forms. Many grazing animals of arid areas prefer this species because of fleshy leaves, high protein and low fiber content during both dry and wet periods (Louhaichi et al., 2021). Since it is widely distributed in water deficit regions and therefore exhibits great potential to cope with the stresses prevailing in these regions by various strategies. Major strategies include biomass maintenance by energy redistribution from growth to tolerance through osmotic adjustment, ion homeostasis and reducing oxidative damages (Dhief et al., 2022).

Physio-anatomical studies are not only of eco-taxonomic significance, but also important for assessing phenotypic plasticity for adaption to environmental heterogeneity. In this context, it was hypothesized that the anatomical adaptations triggered in *S. plumosa* growing under hyperarid environments should have direct modulation on physiological processes to cope with the adverse effects of drought stress by maintaining growth and enhance survivorship. The research questions addressed in this study included an investigation of the impact of soil moisture deficit the physiological attributes; how these attributes help in adaptation to these arid regions; and what structural and functional mechanisms are involved in the adaptability of *S. plumosa* in arid environments.

2. Materials and methods

2.1 Study area

Four water deficit habitats were selected for sampling in different parts of arid regions Punjab, Pakistan including Salt Range, Thal and Cholistan desert. In each habitat, six sites (replicates) were selected at a distance of 500 m. Neela Wahn and Kallar Kahar habitats had dryness ratio (8.40 and 8.90), annual rain falls (519 and 485 mm), sandy loam soil, EC (6.1–7.3 dS m^{-1}), moisture content (3.4% and 3.0%), sodium ion (0.025 and 0.027 g/kg) and potassium ion (0.012 and 0.024 g/kg). Noorpur Thal and Cholistan habitats with dryness ratio (10.90 and 30.49), annual rainfall (400 and 143 mm), sandy clay loam soil and fine sand, EC (8.7–10.7 dS m^{-1}), moisture content (2.8% and 1.8%), sodium ion (0.028 and 0.032 g/kg) and potassium ion (0.018 and 0.061 g/kg). Habitat details along with pictorial views of study sites are presented in Table 1 and Figure 1.

2.2 Determination of dryness of each habitat

The data for mean annual precipitation (P) and mean annual temperature (T) were obtained from Pakistan Meteorological Department weather stations. Mean annual net solar radiation (R) was estimated using daily solar radiations as reported by Adnan et al. (2017). Latent heat of vaporization of water (L) is a constant. Budyko-Lettau dryness ratio (D) was calculated according to Lettau (1969) as $D = (\frac{R}{PxL})$ The D values were used to classify the habitat types following the criteria given by Hare (2019) (Table 1).

2.2.1 Budyko-Lettau Dryness ratio (D)

Dryness ratio was calculated according to Budyko (1958) by the following formula

$$D = (\frac{R}{PxL})$$

Where, **D** = dryness ratio, **R** = mean annual net radiation (i.e. approx. 985,500 J m^{-2} s^{-1}), **P** = Precipitation, **L** = latent heat of vaporization of H_2O

The D values were used to classify the habitat types following the criteria given by Hare (1985). See introduction for details of classification.

2.2.2 Air Soil moisture deficit Index (MDI_{Air})

MDI_{Air} was calculated by the following formula devised by considering the temperature (T) and mean annual net radiation (R) as the main factors restricting precipitation (P) and latent heat of vaporization (L) (Nathan and Sinha, 1996).

$$MDI_{Air} = \frac{(PxL)}{(TxR)}$$

2.2.3 Soil Evaporative Stress Index (ESI_{soil})

As the mean maximum temperature (T) and the mean annual net radiation (R) exerting evaporative stress on the

Table 1. Meteorological data and soil characteristics (at depth 12 cm) of *Stipagrostis plumosa* L. collected from various arid habitats with varying dryness ratio.

Parameters	**NeW**	**KKr**	**NpT**	**Cho**
GPS Coordinates				
Latitude (N)	32°39'55.39"	32°36'00.1"	31°58'02.88"	28°41'56.6"
Longitude (E)	72°37'11.70"	72°26'52.7"	72°12'46.05"	71°19'00.8"
Elevation (m a.s.l.)	833	506	187	103
Climatic data				
Dryness ratio (D)*	8.40	8.99	10.90	30.49
UNESCO classification based on (D) **	Desert	Desert	Extreme desert	Extreme desert
MDI_{Air}	252.06	278.72	425.16	1280.74
ESI_{Soil}	0.35	0.45	0.61	1.02
Mean Annual Rainfall (mm)	519	485	400	143
Mean Annual Temp. (°C)	12	17	22	28
Max. Annual Temp. (°C)	32	36	39	42
Min. Annual Temp. (°C)	-1	0	2	4
Humidity (%) Oct 2016	43	36	21	18
Wind speed (Km h^{-1}) Oct 2016	18	19	22	26

* Calculated after Lettau (1969)
** Classification based on UNESCO (1979)
Sites abbreviations: NeW: Neela Wahn; KKr: Kallar Kahar; NpT: Noorpur Thal; Cho: Cholistan
Abbreviations: D: Budyko-Lettau dryness ratio; MDI Air: Air soil moisture deficit index; ESI Soil: Soil evaporative stress index

soil by decreasing its moisture (M) and increasing latent heat of vaporization of water (L), a formula was created to calculate ESI_{soil} (Yang et al., 2018).

$$ESI_{soil} = \frac{(MxL)}{(TxR)}$$

2.3 Analysis of soil samples

Plants from each study area were uprooted with a soil auger. Soil moisture content (% w/w) was calculated as the difference between final weight and initial weight divided by the initial weight of sample and multiplied by 100 (Sparks, 1996). Soil texture was recorded by hydrometer method (Gavlak et al., 2005) while soil textural class was assigned using the USDA textural triangle. Organic matter was determined according to the method of Walkley (1947). A saturation paste of the soil was prepared and used to analyze various attributes of soil such as pH and EC by using a combined pH and EC meter (WTW series InoLab pH/Cond 720, USA). The concentration of various ions such as Na^+, K^+ and Ca^{2+} was determined from saturation paste by flame photometer (Jenway, PFP–7, UK). The Mg^{2+} content was determined by using atomic absorption spectrophotometer (Perkin Elmer/AA-300, Germany) while Cl^- content was estimated via Mohrs' titration method. Nitrogen content was estimated by micro-Kjeldahl method using the UDK-132 semiautomatic ammonia distillation unit (NIB-B (3)-DSU-003). Soil available phosphorus was determined by using protocol of Yoshida et al. (1971) (Table 2).

2.4 Experimental layout

Repeated visits (four) were conducted on same site (as identified with GPS tags) during the active growing season of this species for the collection of soil sampled and the data was averaged to make one replicate. Five average-sized plants from each site (subreplicates/repeats) growing under open sun in full light intensity were randomly selected and their data was averaged to constitute one replicate. Since it was a study on natural populations, the plants of almost the same age and average size were selected using morphological observations and root:shoot allometric functions.

2.5. *Stipagrostis plumosa* habit and economic importance

Stipagrostis plumosa is a perennial grass widespread in the desert, where it is important as fodder and also as a stabilizer of sand dunes. It grows in dense tufts up to 60 cm high and stems branches densely from the base. The fine, silvery leaf blades are 15 cm long and curled. Silvery flowers are born on panicles up to 15 cm in length throughout the year. The junction of leaf and leafstalk is a

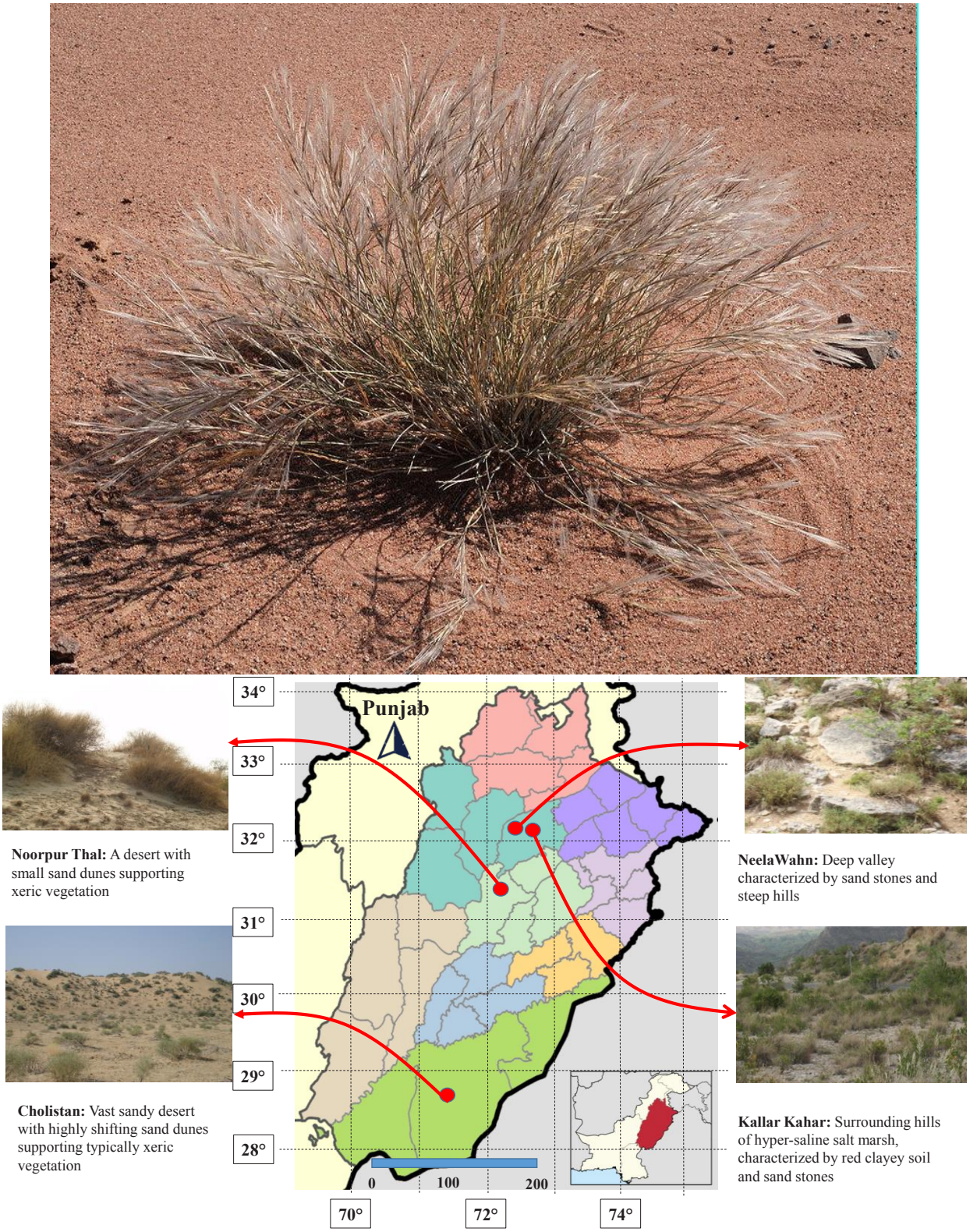

Figure 1. Pictorial view of *Stipagrostis plumosa* L. and habitat details of the collection sites.

Table 2. Soil characteristics (at depth 12 cm) of *Stipagrostis plumosa* L. collected from various arid habitats with varying dryness ratio.

Parameters	NeW	KKr	NpT	Cho	F-ratio	LSD
Soil physico-chemical properties						
Soil texture	LS	SL	SCL	FS		
Amount of sand (%)	80	75	65	85		
Amount of silt (%)	12	15	13	10		
Amount of clay (%)	08	10	22	05		
Soil pH	7.7 ± 0.52^{c}	8.2 ± 0.26^{b}	9.5 ± 0.49^{a}	7.9 ± 0.15^{bc}	52.2^{***}	0.36
EC (dS m^{-1})	6.1 ± 0.28^{d}	7.3 ± 0.66^{c}	8.7 ± 0.43^{b}	10.7 ± 0.60^{a}	7.6^{**}	2.05
Organic matter (%)	0.11 ± 0.03^{c}	0.58 ± 0.01^{a}	0.40 ± 0.01^{b}	0.52 ± 0.02^{a}	73.8^{***}	0.07
Moisture content (%)	3.6 ± 0.11	3.0 ± 0.06	2.8 ± 0.04	1.8 ± 0.05	ns	1.94
Saturation percentage (%)	34 ± 2.3^{c}	44 ± 1.9^{a}	40 ± 2.2^{b}	30 ± 3.1^{d}	5.33^{*}	6.65
Extractable ions						
Na^{+} (g/kg)	0.025 ± 1.17^{d}	0.027 ± 2.14^{c}	0.028 ± 1.75^{b}	0.032 ± 1.99^{a}	220.1^{***}	2.66
K^{+} (g/kg)	0.012 ± 1.11^{d}	0.024 ± 1.76^{b}	0.018 ± 1.95^{c}	0.061 ± 2.45^{a}	51.8^{***}	1.88
Ca^{2+} (g/kg)	0.014 ± 0.99^{a}	0.010 ± 1.0^{b}	0.004 ± 0.56^{c}	0.003 ± 0.11^{c}	40.3^{***}	2.71
Mg^{2+} (g/kg)	0.0004 ± 0.09^{b}	0.0003 ± 0.05^{c}	0.0005 ± 0.08^{a}	0.0003 ± 0.05^{d}	66.3^{***}	0.03
PO_4^{-3} (g/kg)	0.0001 ± 0.003^{a}	0.0002 ± 0.006^{a}	0.0001 ± 0.007^{b}	0.0002 ± 0.004^{a}	10.8^{**}	0.01
Cl^{-} (g/kg)	0.0027 ± 0.16^{a}	0.0023 ± 0.14^{a}	0.0014 ± 0.19^{b}	0.0013 ± 0.14^{b}	9.14^{**}	0.72
NH_4-N (g/kg)	0.0004 ± 0.02^{a}	0.0004 ± 0.01^{a}	0.0002 ± 0.02^{c}	0.0003 ± 0.04^{b}	26.8^{***}	0.07
NO_3-N (g/kg)	0.00004 ± 0.002^{b}	0.00019 ± 0.009^{a}	0.00006 ± 0.006^{b}	0.00003 ± 0.004^{b}	48.35^{***}	0.03

Mean for soil physico-chemical properties are provided with ± SE values. n = 5
Sites abbreviations: NeW: Neela Wahn; KKr: Kallar Kahar; NpT: Noorpur Thal; Cho: Cholistan
Abbreviations: LS: Loamy Sand; SL: Sandy Loam; SCL: Sandy Clay Loam; FS: Fine Sand; MC: Moisture content; D: Budyko-Lettau dryness ratio; MDI Air: Air soil moisture deficit index; ESI Soil: Soil evaporative stress index
*, **, ***: Significant at 0.05, 0.01 and 0.001 levels, respectively. Means sharing same letters within habitats are nonsignificant at $p \leq 0.05$.

dense fringe of hairs. The feathery glumes at the base of the spikelets remain for a long time. It grows on shallow stable sands and sandy silt soils, and is highly salt tolerant. It is rangeland grass and is recommended for land reclamation and restoration of desert forage resources (Figure 1).

2.6 Analysis of plant samples

2.6.1 Morphological traits

Plants were uprooted from the soil and washed. The data for both shoot and root fresh biomass was recorded immediately using an electronic digital balance. After recording fresh weight plants were kept in an oven for three days at 65 °C to record the dry biomass. Leaf area was calculated using the formula of Lopes et al. (2016).

Total leaf area = Maximum leaf length × Maximum leaf width × Correction Factor (i.e. 0.68)

2.6.2 Physiological traits

Photosynthetic pigments

Chlorophyll (*a, b*) and carotenoids contents were assessed via procedure of Arnon (1949) and Davis (1976), respectively.

Anti-oxidative enzymes

For extraction of antioxidative enzymes, fresh leaf tissue 0.25 g was put in 10 mL K_2HPO_4 extraction buffer, and after centrifugation, supernatant was used to evaluate the enzymatic antioxidants activities (Dixit et al., 2002). Giannopolitis and Ries (1977) procedure was followed for measurement of superoxide dismutase (SOD). For the estimation of catalase (CAT) and peroxidase (POD) method of Chance and Maehly (1955) was adopted. For the measurement of ascorbate peroxidase (APX), method of Nakano and Asada (1981) was adopted.

Organic osmolytes

The procedure as ascribed by Bates et al. (1973) was followed to estimate free proline. Glycinebetaine was recorded via protocol of Greive and Grattan (1983). Total soluble proteins were assessed via method of Bradford (1976). Total soluble sugars were determined using protocol optimized by Rose et al. (1991). Hamilton and Van-Slyke (1973) method was followed to measure the total free amino acids.

2.6.3 Inorganic elements analysis

Plant material (0.1 g) was acid-digested (H_2SO_4:H_2O_2 method) for the estimation of ions following the method of (Wolf, 1982). The same protocols and instrumentation as described above for soil analysis was adopted for inorganic element's concentration (Na^+, K^+, Ca^{2+} and Mg^{2+}) in plant tissues. The Na^+, K^+ and Ca^{2+} were determined using a flame photometer (PFP-7, Jenway) while Mg^{2+} was determined on an atomic absorption spectrophotometer (AAnalyst-300, Perkin Elmer, Germany). Soil available phosphorous (as PO_4^{3-}) was estimated spectrophotometrically using UV-Visible spectrophotometer (Hitachi 220, Japan) following Yoshida et al. (1971) while NO_3^- according to the method of Kowalenko and Lowe (1973).

2.7 Anatomical traits

All populations of *S. plumosa* were collected and washed with tap water and then with distilled water before measuring anatomical parameters. A stem piece measuring 1.5 cm from the center of the top internode was taken for stem anatomy, a 1.5 cm piece of flag leaf separated from the leaf-base adjoining to leaf sheath for leaf and leaf sheath anatomy, and a piece of root from the base up to 2.5 cm length was preserved for anatomical studies. A formalin acetic alcohol (v/v formalin 10%, acetic acid 5%, ethyl alcohol 50% and distilled water 35%) was used for fixation and acetic alcohol (v/v acetic acid 25%, and ethanol 75%) solution for preservation. Permanent slides were prepared following the safranin-fast green staining technique following Ruzin (1999). Micrographs of stained sections were taken on a digital Nikon FDX-35 camera equipped with a Nikon 104 stereo-microscope. An ocular micrometer calibrated with a stage micrometer was used for taking measurements. Area and thickness of tissues like epidermis, parenchyma, sclerenchyma, mesophyll, bulliform cells, and vascular tissue were recorded. Other anatomical characteristics of dermal tissue (epidermis, endodermis) parenchymatous tissue (mesophyll, cortex, pith) and conducting tissue (metaxylem, phloem) were also measured. The measurement details of various tissues are presented in Figure 2.

2.8 Statistical analysis

The data were analyzed statistically using analysis of variance (ANOVA) with Costat (Cohort 6). The Fishers least significant difference (LSD) values (5%) were computed and used to determine the significance of mean values. A polynomial regression line was fitted to predict the trend in different plant attributes along with increasing soil moisture deficit. Heatmap clustering was performed with a customized code using R Studios Version 1.1.463 backend by R version 4.0.3 (The R Foundation for Statistical Computing, 2020). Ecological analysis was performed with CANOCO (4.5 version) software. The redundancy analysis (RDA) was calculated by estimating the response of the plants' morphological attributes (response variable as factor 1) against the soil physiochemical attributes (independent variables as factor 2) of the study sites (fixed variables as factor 3). The RDA was run with the following settings: scaling of data to inter-parameter correlations; division of parameter score by standard deviation; no data transformation or forward selection; parameters centered and standardized by attribute; study areas centered by sites. The RDA triplots for all three factors outlined above were then constructed in CanoDraw software (version 4.14, ter Braak and Smilauer, 2002)

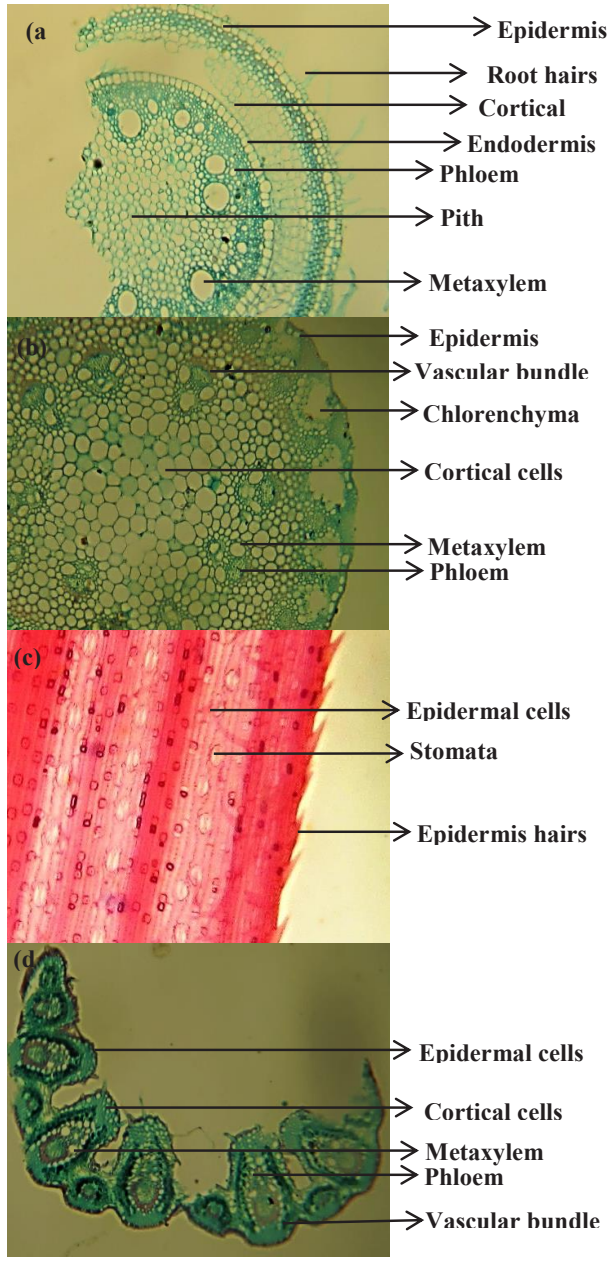

Figure 2. Measurement details of root (a), stem (b), leaf epidermis (c), and leaf mid rib (d) anatomical traits of *Stipagrostis plumosa* L.

supplied with Canoco software. To evaluate the response of various plant attributes against increasing moisture gradients (from 1% to 4.5 %), a GLM (Generalized Linear Model) was fitted to generate the response curves of the plant traits. The following model settings were used: linear degree; binomial distribution; and, maximum binomial total. All attributes exhibiting collinearities in datasets were excluded from GLM response models. The visualization of response curves was then performed with CanoDraw software.

As described by Wellband and Heath (2017), the plasticity of various attributes along increasing moisture gradients was described by a generalized linear model (GLM). The variables showing a zero slope in GLM (those that remained unaltered in all habitat types and included in the model as straight lines) or co-linearity in the regression model (those attributes indicating linear response to moisture gradient and were excluded from the model) at all moisture levels were nonplastic attributes. The variables exhibiting positive slopes were positively plastic as they responded directly to increasing moisture gradient (as shown by direction of arrow in figures). Those variables exhibiting negative slopes in GLM were negatively plastic as they responded inversely to moisture deficit. The strength of plasticity was directly proportional to the curvature of slopes generated in GLM model.

3. Results

The root to shoot length ratio increased along the increasing dryness ratio. Smaller leaf area was observed in Cholistan (Cho) populations in comparison to the Neela Wahn (NeW) and Kallar Kahar (KKr) populations. Above (shoot fresh and dry weight ratio) and below (root fresh to dry weight ratio) ground biomass showed a significant decrease in populations with increasing dryness ratio (Figure 3). Populations from Noorpur Thal (NpT) and Cholistan (Cho) deserts showed relatively higher chlorophyll *a* and carotenoid content in comparison to the NeW and KKr populations while Chl *b* showed nonsignificant association with aridity (Figure 4).

Shoot and root Ca^{2+} content decreased significantly along the increasing dryness ratio. Maximum calcium was recorded in NeW and KKr populations from the

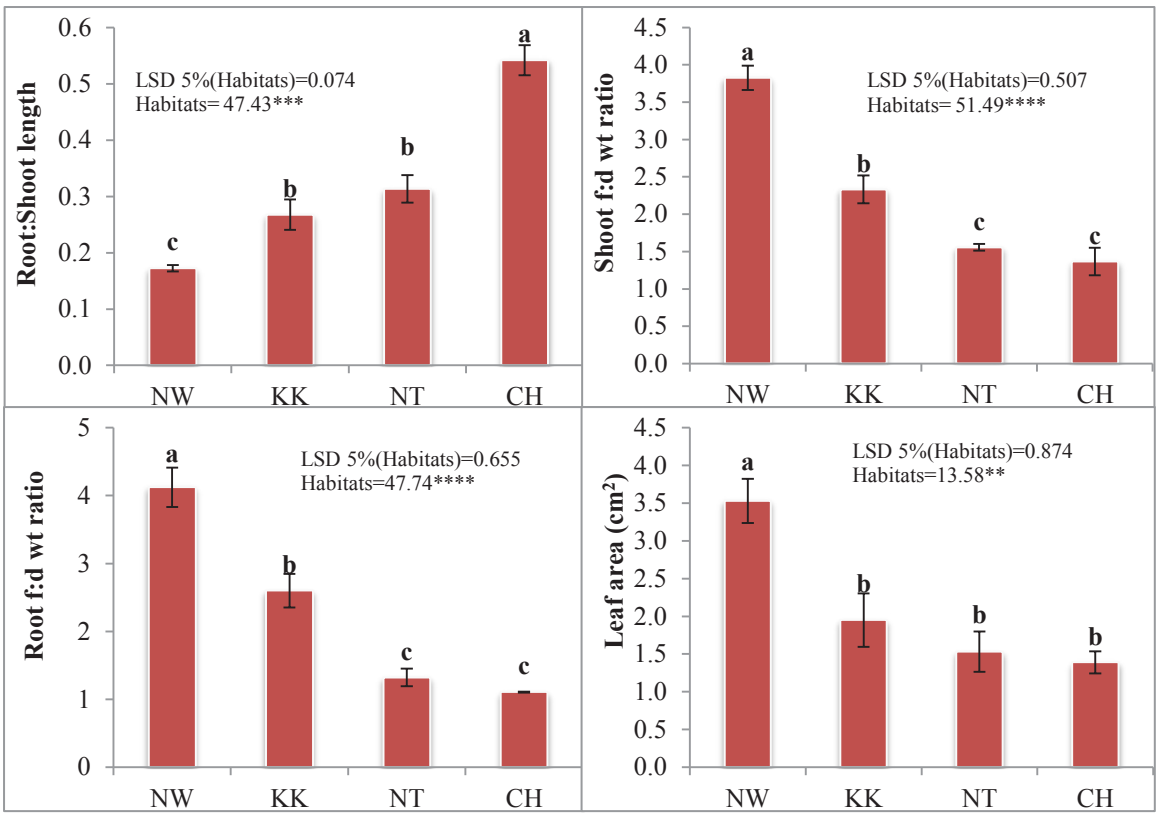

Figure 3. Mean values of morphological attributes of the *Stipagrostis plumosa* L. collected from arid habitats. Habitats were arranged according to decreasing precipitation and increasing dryness ratio from left (being the less arid) to right (being more arid). Polynomial regression lines were fitted to predict the possible trend in different plant attributes along increasing soil moisture deficit. **, ***: Significant at 0.01 and 0.001 levels, respectively. Bars sharing same letters within habitats are nonsignificant at $p \leq 0.05$.

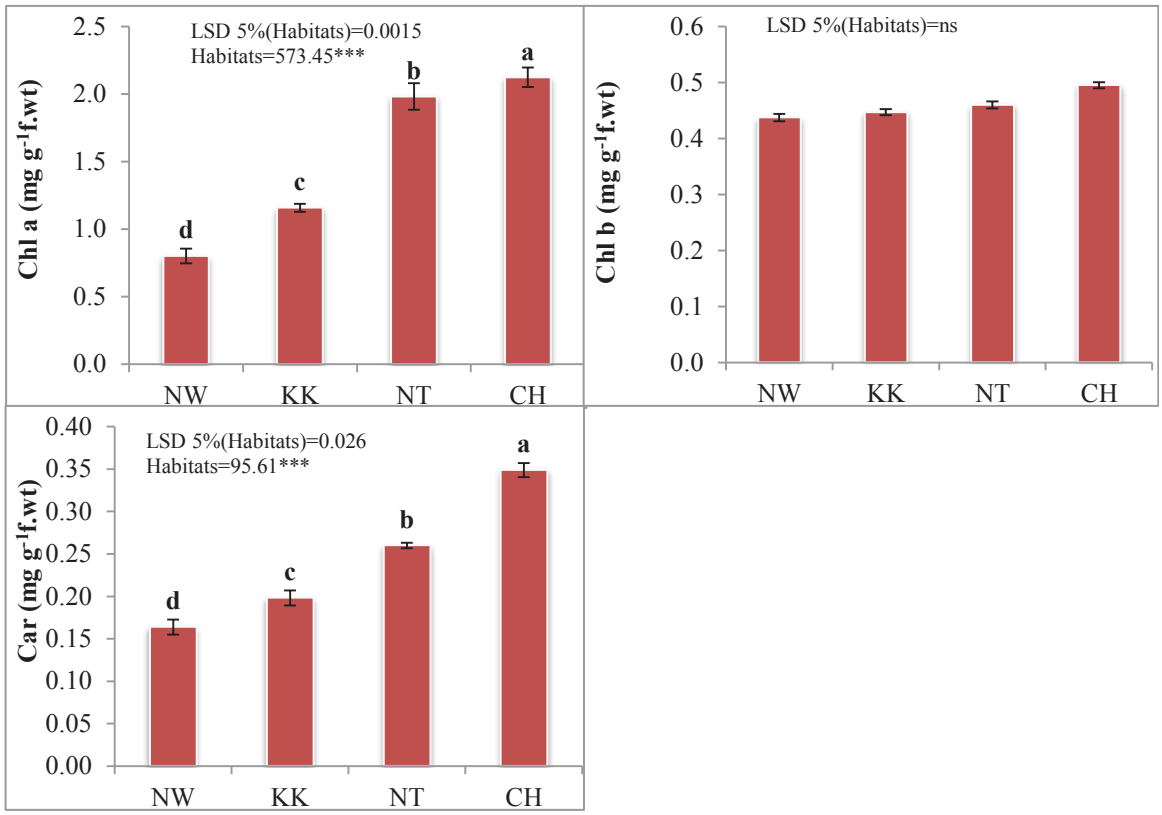

Figure 4. Mean values of photosynthetic pigments of the *Stipagrostis plumosa* L. collected from arid habitat. Habitats were arranged according to decreasing precipitation and increasing dryness ratio from left (being the less arid) to right (being more arid). Polynomial regression lines were fitted to predict the possible trend in different plant attributes along increasing soil moisture deficit. ***: Significant 0.001 level. ns= not significant. Bars sharing same letters within habitats are nonsignificant at $p \leq 0.05$.

relatively less-arid habitat in both root and shoot tissues. Potassium and sodium content of both tissues increased significantly along the increasing dryness ratio. Both ions were high in NpT and Cho populations (Figure 5). Shoot and root magnesium and phosphorus contents enhanced significantly along the increasing dryness ratio. The NpT and Cho populations showed more magnesium and phosphorus contents in both tissues. Populations from NeW and KKr exhibited high nitrogen in shoot as compared to root (Figure 6).

Organic osmolytes such as total soluble proteins, total free amino acids, glycinebetaine and proline showed the highest accumulation in hyperarid NpT and Cho populations while total soluble sugars were nonsignificantly different (Figure 7). Activities of antioxidants such as ascorbate peroxidase (APX), catalase (CAT), peroxidase (POD) and superoxide dismutase (SOD) were the highest in NpT and Cho populations while low activities were recorded in NeW and KKr populations (Figure 8).

Root epidermis, cortical region and endodermis thickness decreased significantly along the increasing dryness ratio. The NeW and KKr populations exhibited thick epidermis, cortex and endodermis as compared to the NpT and Cho populations. Largest cortical cell area was recorded in NeW and KKr populations with significant decrease in NpT and Cho populations. Metaxylem area, phloem area and pith area exhibited a significant decrease in NpT and Cho populations from hyperarid environments (Table 3; Figure 9).

Leaf epidermal cell area increased significantly along the increasing dryness ratio. The NeW and KKr populations exhibited thick epidermis and large cortical cell area as compared to the NpT and Cho populations. Significantly larger metaxylem and phloem areas were produced in NpT and Cho populations (Table 3; Figure 10). Abaxial stomatal density decreased while stomatal area increased along the increasing dryness ratio. NpT and Cho populations showed higher number of stomata with large stomatal area on abaxial side (Table 3; Figure 11). Thick stem epidermis with large cortical cell area was recorded in NpT and Cho populations. Metaxylem area increased significantly along the increasing dryness ratio. Large metaxylem and small phloem areas were observed in NpT and Cho populations (Table 3; Figure 12).

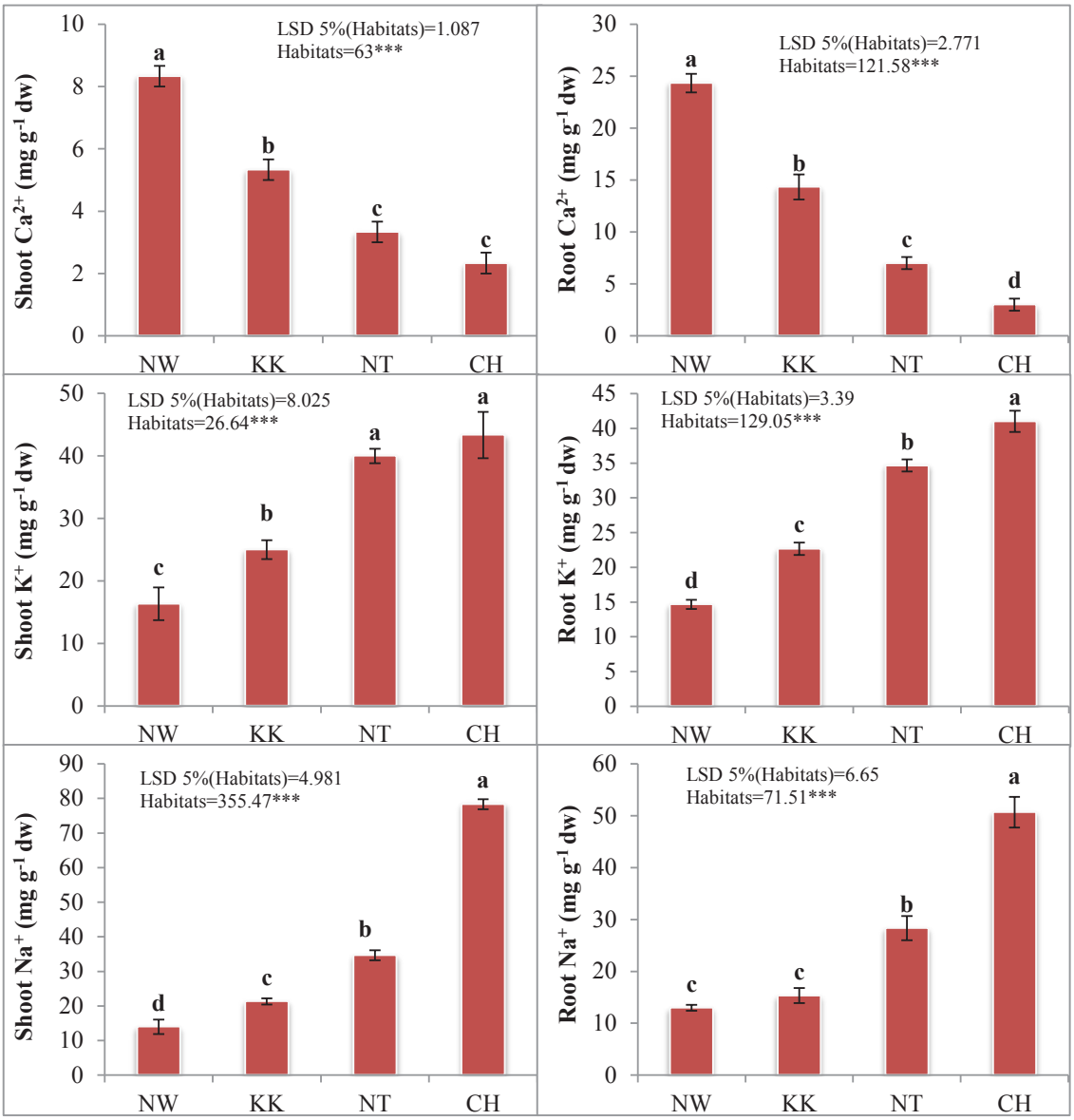

Figure 5. Mean values of Ca^{2+}, K^+ and Na^+ content for shoot and root of the *Stipagrostis plumosa* L. collected from arid habitats. Habitats were arranged according to decreasing precipitation and increasing dryness ratio from left (being the less arid) to right (being more arid). Polynomial regression lines were fitted to predict the possible trend in different plant attributes along increasing soil moisture deficit. ***: Significant at 0.001 level. Bars sharing same letters within habitats are nonsignificant at $p \leq 0.05$.

RDA triplot for morpho-physiological attributes of *S. plumosa*

Redundancy analysis (RDA) triplots for morpho-physiological traits showed that soil moisture content was strongly associated with the leaf area and root fresh to dry weight ratio while chlorophyll (Chl *a* & Chl *b*) were linked to the potassium and electrical conductivity (EC) of soil. Calcium content of both shoot and root (S-Ca, R-Ca) were linked with NH_4 of Neela Wahn (NeW) habitat. In Kallar Kahar (KKr) habitat, soil magnesium content was strongly influenced by root magnesium (R-Mg) content. Some ions such as sodium, nitrogen and phosphorus (S-Na, S-N, S-P, R-Na, R-N and R-P) in both tissues were centered in the triplot indicating no relationship with soil attributes. Soil potassium of Neela Wahn (NeW) habitat activated the superoxide dismutase (SOD). Hyperarid habitat Cholistan (Cho) was strongly associated with the moisture contents that activated the ascorbate peroxidase (APX), peroxidase (POD), glycinebetaine (GB) activities and proline accumulation (Figure 13).

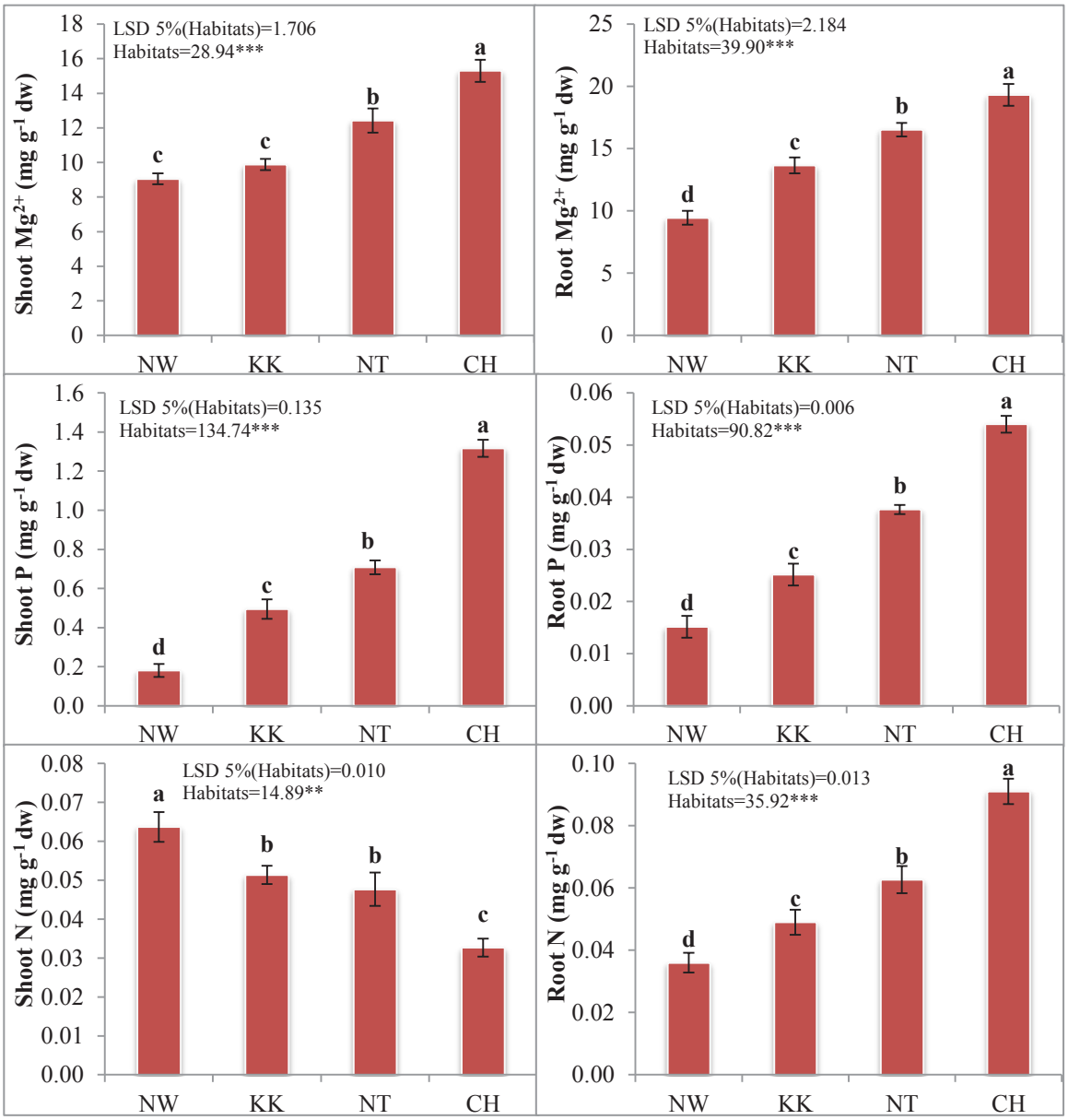

Figure 6. Mean values of Mg^{2+}, P and N content for shoot and root of the *Stipagrostis plumosa* L. collected from arid habitats. Habitats were arranged according to decreasing precipitation and increasing dryness ratio from left (being the less arid) to right (being more arid). Polynomial regression lines were fitted to predict the possible trend in different plant attributes along increasing soil moisture deficit. **, ***: Significant at 0.01 and 0.001 levels, respectively. Bars sharing same letters within habitats are nonsignificant at $p \leq 0.05$.

Response curves for morpho-physiological attributes

Response curves for the morpho-physiological traits showed that leaf area and shoot fresh to dry weight ratio were positively sloped with increasing soil moisture deficit while root to shoot length was negatively slopped. Calcium content of both root and shoot (R-Ca, S-Ca) were positively slopped while potassium, magnesium, and phosphorus of both root and shoot tissue (R-K, R-Mg, S-P, R-P, S-Mg) were negatively slopped with decreasing soil moisture deficit. Root and shoot nitrogen content (R-N, S-N) were plotted linearly indicating no significant link with soil moisture deficit. Total free amino acids and total soluble proteins were negative sloped with increasing soil moisture contents (Figure 13).

Heatmap clustering between growth, physiological attributes and ionic contents

The heatmap clustering showing the influence of soil physico-chemical properties on growth, physiology, ionic

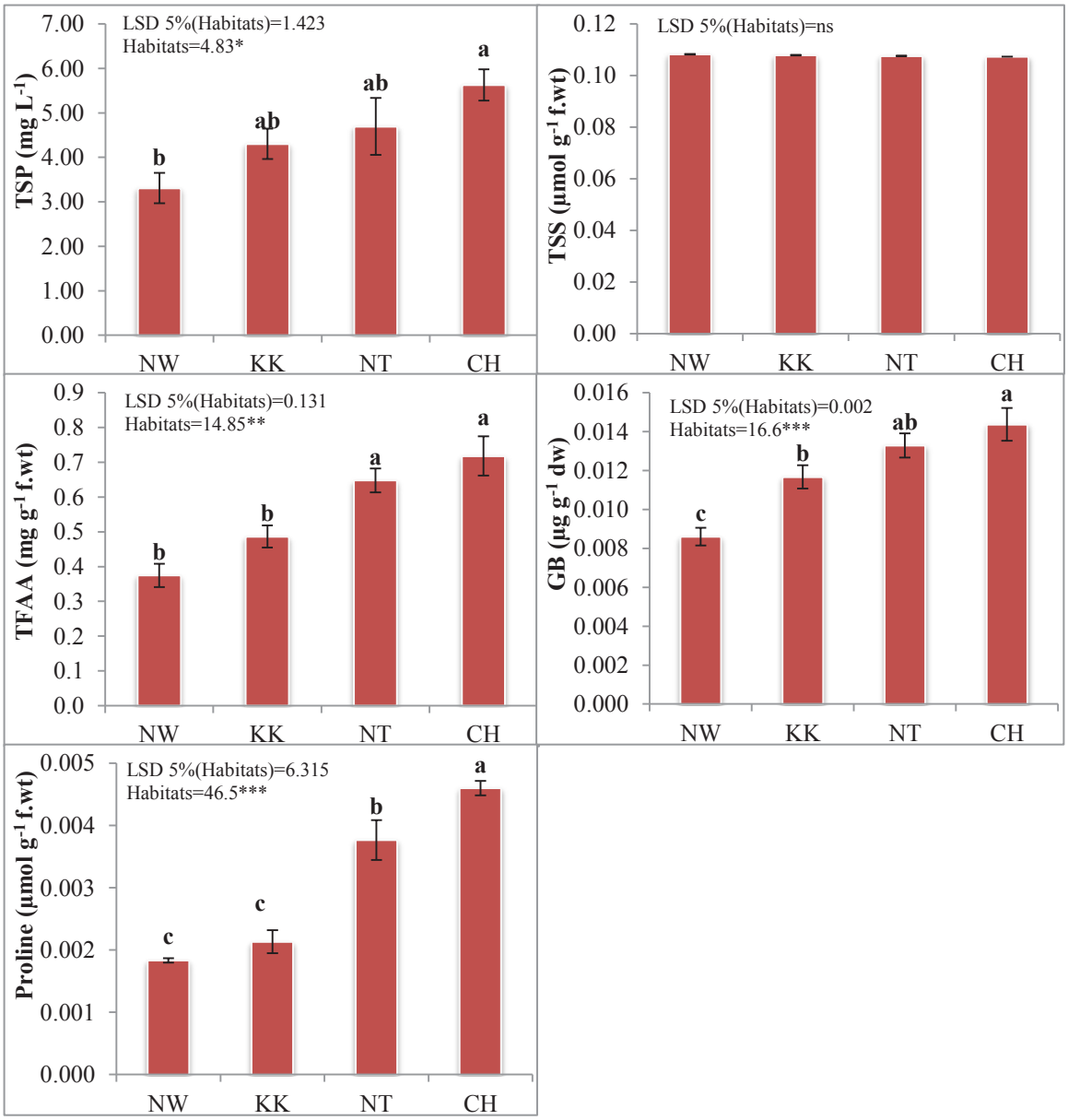

Figure 7. Mean values of organic osmolytes of the *Stipagrostis plumosa* L. collected from arid habitats. Habitats were arranged according to decreasing precipitation and increasing dryness ratio from left (being the less arid) to right (being more arid). Polynomial regression lines were fitted to predict the possible trend in different plant attributes along increasing soil moisture deficit. *, **, ***: Significant at 0.05, 0.01 and 0.001 level, respectively. ns= not significant. Bars sharing same letters within habitats are nonsignificant at $p \leq 0.05$.

contents (root and shoot), and anatomical attributes grouped all four studied populations into two distinct clusters. The two populations NeW and KKr (cluster i) were clustered separately from NpT and Cho (cluster ii) populations indicating similarities in their mechanisms pertaining to long-term growth in their native habitats (Figure 14).

Among ions, nitrogen, phosphorus, sodium, chlorophyll *b*, carotenoids, root:shoot length were plotted in the same subcluster with its sister subcluster containing carotenoid, magnesium and potassium (cluster 1) because of their role in chlorophyll synthesis and functioning. Soil attributes such as nitrate, pH, magnesium and organic matter did not influence any growth attributes and clustered separately. In NeW and KKr populations, the attributes plotted in cluster 1 were strongly negatively and in cluster 2 strongly positively influenced. The NeW and Cho populations showed a strong positive influence for

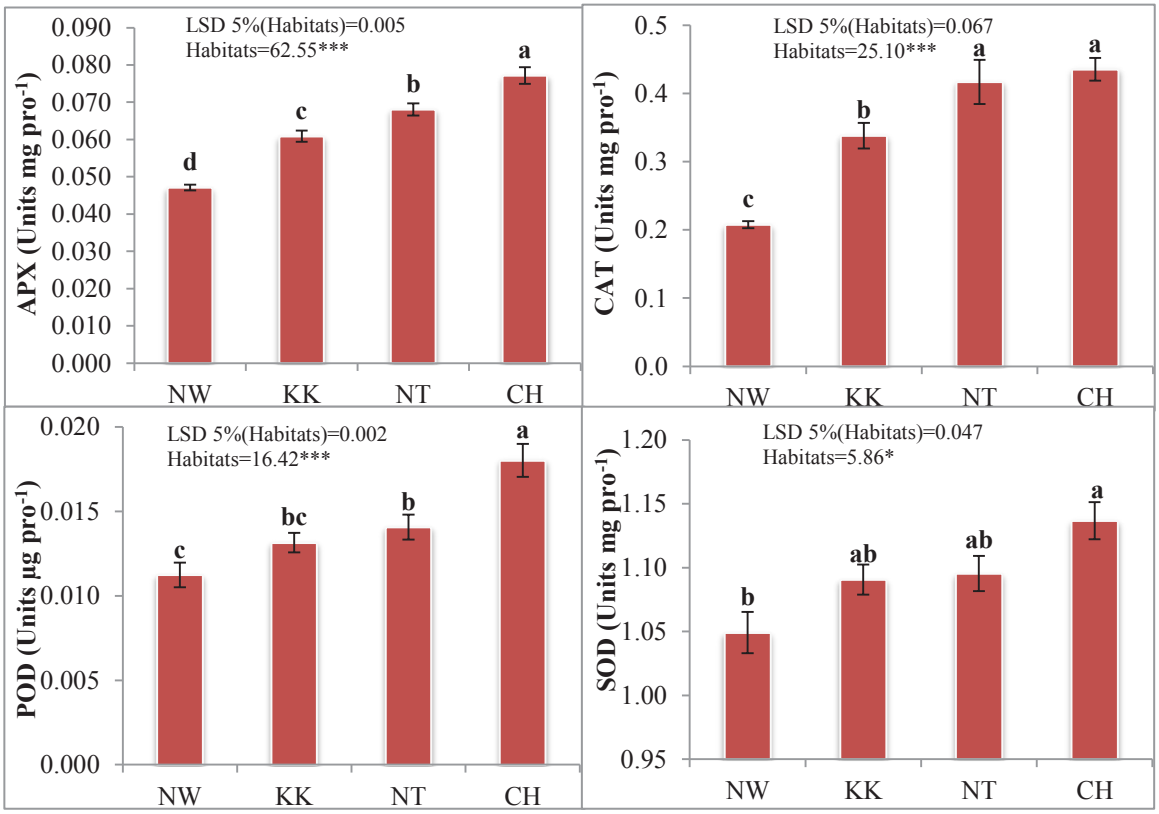

Figure 8. Mean values of enzymatic antioxidant of the *Stipagrostis plumosa* L. collected from arid habitats. Habitats were arranged according to decreasing precipitation and increasing dryness ratio from left (being the less arid) to right (being more arid). Polynomial regression lines were fitted to predict the possible trend in different plant attributes along increasing soil moisture deficit. *, ***: Significant at 0.05 and 0.001 levels, respectively. Bars sharing same letters within habitats are nonsignificant at $p \leq 0.05$.

attributes plotted in cluster 1 and a strong negative with attributes in cluster 2. Among osmolytes and antioxidative attributes, TFAA, proline, GB, SOD, POD,TSP, and Chl b were plotted with root: shoot length in the same subcluster (cluster 1) as they are influenced positively by the soil EC of NpT and Cho habitats (Figure 14).

Among anatomical attributes, leaf epidermal and phloem cell area were clustered together with the root:shoot length, chlorophyll *b*, carotenoids and were positively influenced by the soil EC (Cluster 1). Soil sodium, K and MC negatively influenced the leaf epidermal thickness and cortical cell area (Cluster 2) of NpT and Cho populations. Soil sodium, pH, magnesium, phosphorus, organic matter and nitrates were clustered separately so they did not show any grouping with shoot anatomical attributes (Cluster 2 and Cluster 3). Phloem cell area, carotenoids, chlorophyll *b*, and root:shoot length were positively influenced by the soil EC (Cluster 4) while epidermal cell area was negatively influenced by the soil potassium and MC NpT and Cho habitats (Figure 14).

All root anatomical attributes were grouped together in Cluster 2 while soil and growth attributes were in different Clusters 1, 3, and 4 for both populations. Root fresh to dry weight ratios, shoot fresh to dry weight, leaf area, root endodermal thickness showed a positive influence of NeW and KKr populations. Chlorophyll *a, b*, root:shoot length and carotenoids were influenced by the soil EC of NpT and Cho habitats (Cluster 1). Soil phosphorus, nitrates, saturation percentage, pH and magnesium were not grouped with any root anatomical attributes in both less arid (NeW and KKr) and hyperarid (NpT and Cho) populations (Figure 14).

Heatmap clustering of growth, physiological attributes and ionic contents with climate

Clustered heatmap showing association of climatic factors with various morpho-physiological attributes of different populations of *S. plumosa*. Cluster 1 clustered humidity (Hum) and root fresh:dry weight ratio (RFD) closely with root and shoot calcium, leaf area (LA) and shoot fresh:dry weight ratio (SFD) at New and Cho sites. The root and shoot Ca of KKr population was moderately affected by RFD and Hum. Cluster 2 showed a strong association of climatic factors i.e. maximum and minimum temperatures (MMT, MAT, MIT), and wind speed (WS)

Table 3. Anatomical attributes of *Stipagrostis plumosa* L. collected from various arid habitats with varying dryness ratio.

Parameters	NeW	KKr	NpT	Cho	F-ratio	LSD
Root anatomy						
Epidermis thickness (µm)	51.9^{a}	47.2^{ab}	33.0^{b}	33.0^{b}	4.2*	15.40
Epidermis cell area (µm^2)	3313.0^{a}	2557.5^{b}	1630.2^{c}	946.5^{d}	11.3**	999.99
Cortical region thickness (µm)	665.9^{a}	533.7^{b}	481.7^{c}	472.3^{d}	178.3***	21.78
Cortical cell area (µm^2)	7362.2^{a}	5363.9^{b}	4312.1^{c}	1945.7^{d}	23.8***	1507.32
Endodermis thickness (µm)	108.6^{a}	51.9^{b}	47.2^{bc}	33.0^{c}	49.5***	15.40
Endodermis cell area (µm^2)	6468.2^{a}	3470.7^{b}	3260.4^{c}	841.4^{d}	45.1***	1118.02
Metaxylem area (µm^2)	41754.5^{a}	41176.0^{b}	15408.1^{c}	2471.6^{d}	134.5***	5485.24
Phloem area (µm^2)	315.5^{a}	315.5^{a}	157.7^{b}	157.7^{b}	2.7***	1.79
Pith area (µm^2)	5626.8^{a}	5206.1^{b}	4627.7^{c}	2419.0^{d}	196.4***	332.10
Leaf anatomy						
Midrib thickness (µm)	713.2^{d}	854.9^{c}	968.2^{b}	996.6^{a}	228.9***	27.7
Epidermis thickness (µm)	28.3	28.3	28.3	28.3	ns	
Epidermis cell area (µm^2)	525.8^{d}	578.4^{c}	841.4^{b}	1051.7^{a}	6.6*	309.1
Cortical cell area (µm^2)	577.6^{a}	525.0^{b}	262.9^{c}	262.9^{c}	33.3***	420.0
Metaxylem area (µm^2)	157.7^{d}	4469.9^{c}	5311.3^{b}	8939.8^{a}	120.6***	1071.0
Phloem area (µm^2)	157.7	157.7	157.7	157.7	Ns	
Stomatal density	4.6^{c}	5.6^{b}	6.3^{a}	6.6^{a}	7*	1.0
Stomatal area (µm^2)	33656.0^{a}	27976.5^{b}	25294.6^{c}	23822.1^{d}	46.2***	2079.2
Stem anatomy						
Epidermis thickness (µm)	28.3^{a}	23.6^{b}	14.1^{c}	14.1^{c}	9**	7.7
Epidermis cell area (µm^2)	279.6^{a}	262.9^{b}	210.3^{c}	157.7^{d}	1.2ns	148.5
Cortical cell area (µm^2)	5626.8^{d}	9676.1^{c}	17353.9^{b}	17879.7^{a}	314.5***	1101.4
Vascular bundle area (µm^2)	136201.8^{d}	157762.7^{c}	183004.7^{b}	187737.6^{a}	146.3***	6448.8
Metaxylem area (µm^2)	13672.7^{d}	16459.9^{c}	18195.3^{b}	18405.6^{a}	16.5***	1753.1
Phloem area (µm^2)	157.7	157.7	157.7	157.7	ns	

Sites abbreviations: NeW: Neela Wahn; KKr: Kallar Kahar; NpT: Noorpur Thal; Cho: Cholistan
*, **, ***: Significant at 0.05, 0.01 and 0.001 levels, respectively. ns= not significant. Means sharing same letters within habitats are non-significant at $p \leq 0.05$.

on shoot and root K and Mg, root P, and, Cha and Car of *S. plumosa* at Cho site (Figure 15).

For physiological attributes Cluster 1 showed a strong association of humidity (Hum) at NeW and Cho sites with leaf area, and, shoot and root fresh:dry weight ratio. Other physiological attributes i.e. APX, SOD, TSP, GB, TFA, Cha, and POD were slightly affected by wind speed (WS), temperature (MIT, MMT, MAT) and rainfall (MAR) at NpT site as compared to the other population growing at KKr, Cho and NeW sites. For leaf anatomy, population of *S. plumosa* at Cho and NeW sites were strongly affected by humidity (Hum) showing clustering with leaf cortical cell and pith areas, and, epidermal thickness with mean annual rainfall (MAR). The root:shoot length, photosynthetic pigments (Cha, Chb, and Car), leaf anatomical attributes (epidermal cell and metaxylem areas, midrib thickness, and stomatal density) at NeW and Cho sites were clustered with wind speed (WS) and temperature (MIT, MMT, and MAT). Regarding stem anatomy, the humidity (Hum) at NeW site was strongly related to stem epidermal thickness (SET) while other factors i.e. minimum temperature (MIT) and wind speed (WS) showed a strong association with root:shoot length, Chb, and Car at Cho site as compared to NpT and KKr sites. The stem epidermal (SEC), metaxylem (SMX), and vascular bundle (SVA) areas showed a strong association with minimum (MMT) and mean annual (MAT) temperatures. Clustering of root anatomical attributes represented a strong association of

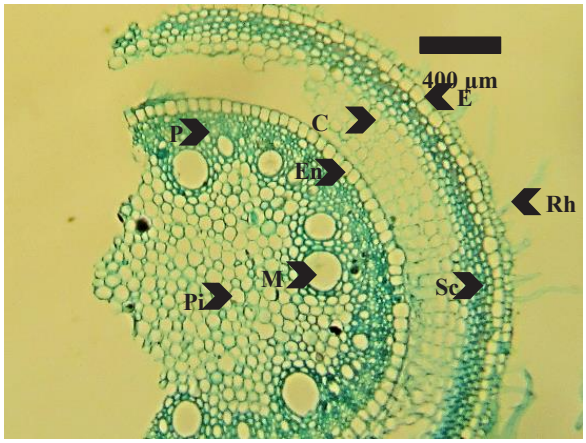

[a) NW] C: Large compactly arranged cortical cells for storage of water, **E:** Some epiblema cells with small root hairs, **En:** Large circular shaped endodermis cells, **M:** Largest metaxylem vessels for efficient transport of water and nutrients protected by sclerenchyma **Rh:** Small epidermal root hairs **Sc:** Intensive **s**clerification in outer cortical region and around vascular connections below endodermis, **Pi:** Large pith cells

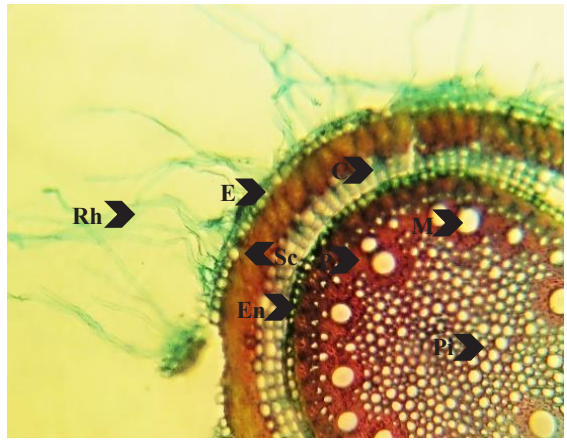

[b) KK] C: Small cortical cells with intercellular spaces, **E:** Epiblema cells with large extensive root hairs, **En:** Small endodermis cells, **M:** Small sized metaxylem vessels with more number **Rh:** Large and extensive root hairs **Sc:** Intensive **s**clerification in outer cortical region and around vascular connections below endodermis, **Pi:** Medium sized pith cells

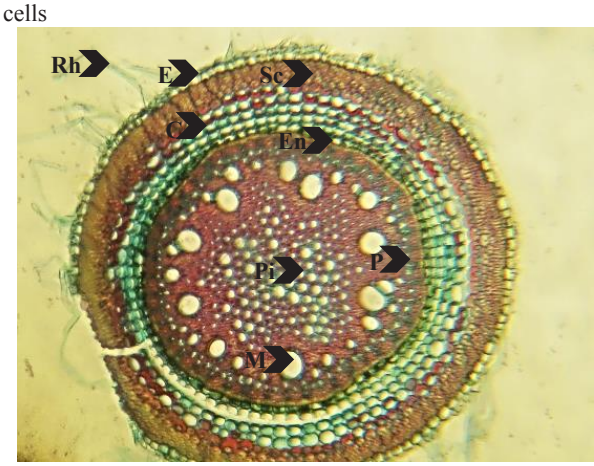

[c) NT] C: Cortical cells with intercellular spaces, **E:** Epiblema cells with medium sized root hairs, **En:** Wavy endodermis with small sized cells, **M:** Medium sized metaxylem vessels **Rh:** Medium sized extensive root hairs **Sc:** Intensive **s**clerification in cortical and around vascular region, **Pi:** Small sized sclerified pith cells

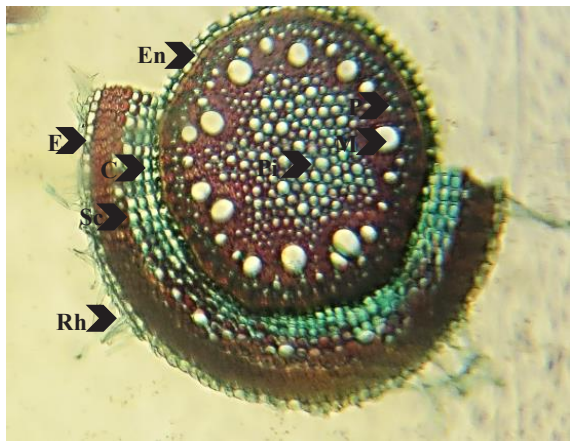

[d) CH] C: Cortical cells with some intercellular spaces, **E:** Epiblema cells with small sized root hairs, **En:** Wavy endodermis, **M:** Large metaxylem vessels **Rh:** Small sized root hairs **Sc:** Intensive sclerification in cortical and vascular region, **Pi:** Small sized sclerified pith cells

Figure 9. Root transverse sections of *Stipagrostis plumosa* L. collected from different sites in the Punjab. All figures are captured at same resolution (40X). Scale bar is given in Figure 9a. Sites abbreviations: NeW: Neela Wahn; KKr: Kallar Kahar; NpT: Noorpur Thal; Cho: Cholistan

humidity (Hum) with root epidermal thickness (RET) at NeW site and a moderate association with root metaxylem (RMX) and phloem (RHA) areas at Cho site. The mean annual rainfall (MAR) at KKr and NpT sites showed less correlation with root pith area (RPA) (Figure 15).

4. Discussion

In arid areas, the root system of plants is considered as the main competitor between species for water uptake as well as their adaptation to water deficit (Kidron, 2019). Over longer time scales, soil moisture deficit tolerant species develop morphological adaptations such as small leaf area, longer root length, and leaf succulence with high water use efficiency (Jan et al., 2019). Variations in root-to-shoot ratio among populations had been reported in arid zones. Root to shoot ratio is enhanced under water deficit due to more allocation of carbohydrates (starch and sugars) towards roots along with the redistribution of photo-assimilates in

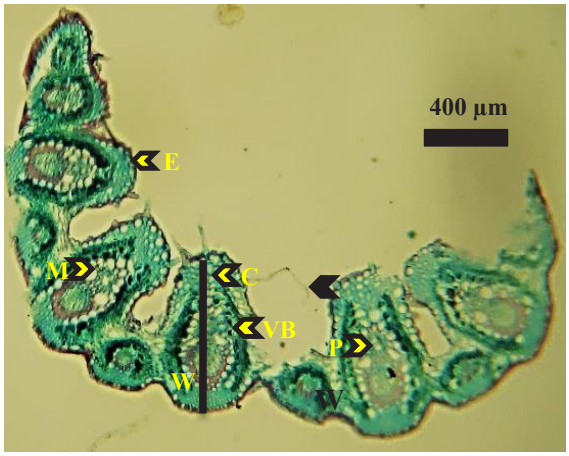

[a) NW] C: Compact arrangement of cortical cells, **E:** Epidermal cells with large hairs **M:** Large metaxylem vessels for efficient transport of water and nutrients, **V:** Large vascular bundle protected by sclerenchyma; **W:** Larger lamina width

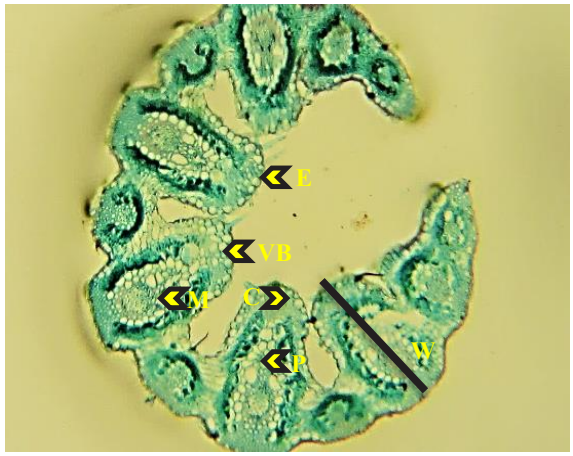

[b) KK] C: Relatively large cortical cells, **E:** Epidermal cells with medium sized sparsely arranged hairs **M:** Large and deformed (non-circular) metaxylem vessels **V:** large vascular bundle with intensive sclerification; **W:** Larger lamina width

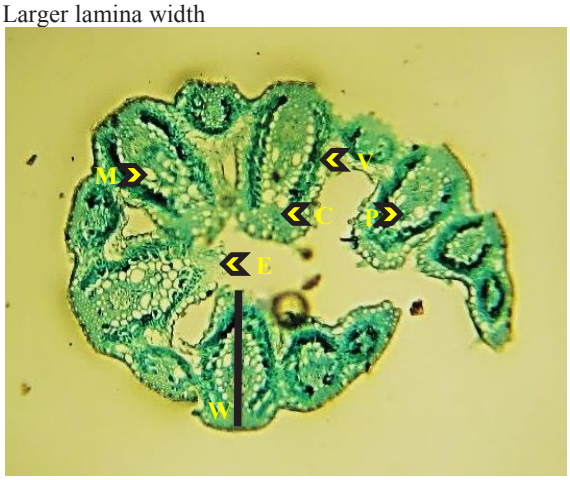

[c) NT] C: Small cortical cells, **E:** Epidermal cells with small sized hairs **M:** Large and deformed metaxylem vessels, **V:** Large vascular bundles protected by sclerenchyma; **W:** Smaller lamina width

[d) CH] C: Small cortical cells, **E:** Epidermal cells with relatively small sparsely arranged hairs **M:** Small and deformed metaxylem vessels, **V:** Small vascular bundle with intensive sclerification; **W:** Smaller lamina width

Figure 10. Leaf midrib transverse sections of *Stipagrostis plumosa* L. collected from different sites in the Punjab. All figures are captured at same resolution (40X). Scale bar is given in Figure 10a. Sites abbreviations: NeW: Neela Wahn; KKr: Kallar Kahar; NpT: Noorpur Thal; Cho: Cholistan

these tissues. Thick and deep root system helps in extraction of water from lower soil depths (Karimpour, 2019; Thapa et al., 2019). The present study reported that root-to-shoot length increased along the increasing dryness ratio. Longer roots were observed in NpT and Cho populations in comparison to the NeW and KKr populations. Above (shoot fresh and dry weight ratio) and below (root fresh to dry weight ratio) ground biomass showed a significant decrease in populations with an increasing soil dryness ratio. Under water deficit conditions, a gradual reduction in growth rate and leaf area was observed which regulates rate of transpiration and plant water fluxes. Smaller leaf area was observed in hyperarid populations from NpT and Cho in comparison to the large leaf area for a relatively less arid NeW population.

Osmotic adjustment is vital for normal functioning of cell and plant growth under water stress (Zhuang et al., 2015; Chavoshi et al., 2018; Masouleh et al., 2019). Osmolytes defend the cellular structures to minimize oxidative stress in response to reactive oxygen species under stress conditions. The main function of osmolytes is to decrease the osmotic potential and hence, modulate the plant water potential to enhance water uptake under water deficit conditions. Hyper accumulator plants produce

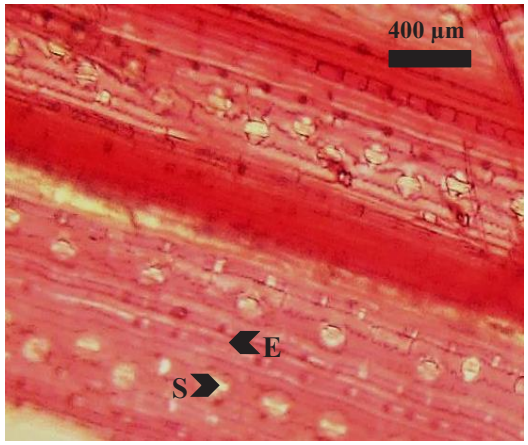

[a) NW] E: Large epidermis cells with intensive sclerification and presence of silica bodies, **Eh:** Epidermal hairs are absent, **S:** Large stomatal area with less number of stomata,

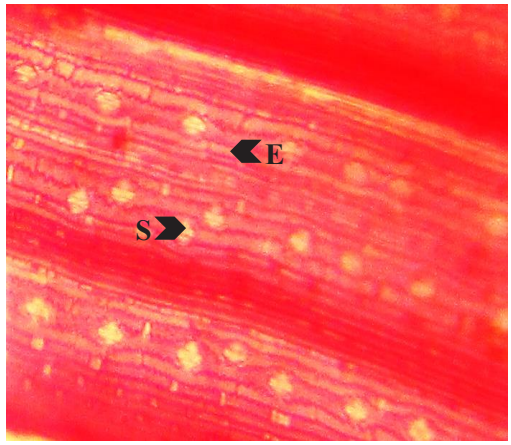

[b) KK] E: Epidermis cells with intensive sclerification and highly invaginated cell walls, **Eh:** Epidermal hairs are absent, **S:** Large stomatal area with increased stomatal density and silica bodies

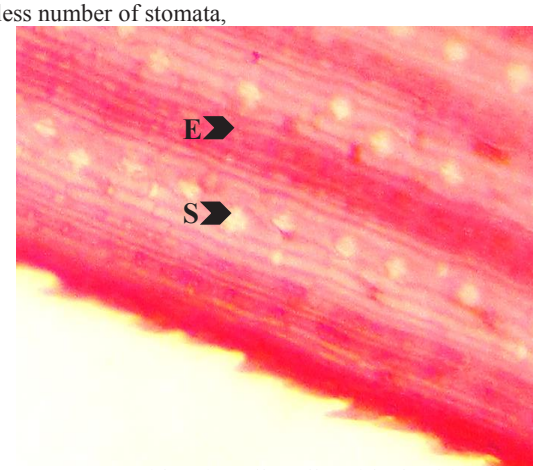

[c) NT] E: Epidermis cell walls with dendrite shaped invaginations, **Eh:** Large epidermal hairs to reduce the transpiratonal loss by wind, **S:** Small stomatal area with more number of stomata

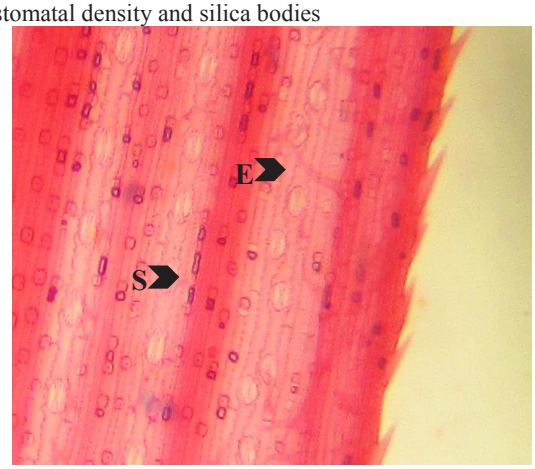

[d) CH] E: Epidermis cell walls with small invaginations at one side, **Eh:** Small epidermal hairs to reduce the transpiratonal loss by wind, **S:** Largest stomatal area with increased stomatal density

Figure 11. Leaf epidermis surface view of *Stipagrostis plumosa* L. collected from different sites in the Punjab. All figures are captured at same resolution (40X). Scale bar is given in Figure 11a. Sites abbreviations: NeW: Neela Wahn; KKr: Kallar Kahar; NpT: Noorpur Thal; Cho: Cholistan

various types of organic osmolytes i.e. amino acids, sugars, and proline that act as signaling molecule and defend plant cells from oxidative damage, ion leakage and membrane stabilization to maintain cell turgidity (Zahoor et al., 2018; Arif et al., 2020). Organic osmolytes such as total soluble proteins, total free amino acids, glycinebetaine and proline were higher in NpT and Cho populations along with the activities of antioxidant enzymes such as ascorbate peroxidase (APX), catalase (CAT), peroxidase (POD) and superoxide dismutase (SOD).

In this study, water deficit caused a significant increase in Na^+ ion in the root and shoot of populations from hyperarid areas i.e. NpT and Cho. Usually, it has been reported that plants growing in saline arid environment absorb higher amount of sodium along with a lower amount of potassium and calcium ions. For cell membrane integrity, a reasonable amount of potassium and calcium ions is essential by plants grown under water deficit (Sun et al., 2018). Both root and leaf K^+ and Na^+ concentration increased while Ca^{2+} content decreased in NpT and Cho populations.

Anatomical traits are more adaptive to environmental conditions, enabling plants to survive under water deficit. Increase in root cortical cells (storage parenchyma) ensures water conservation in dry environments. The presence of sclerified cells around the root vascular and cortical regions maintains root growth and facilitates water absorption in water deficit conditions (Moris et al., 2018). Root epidermal

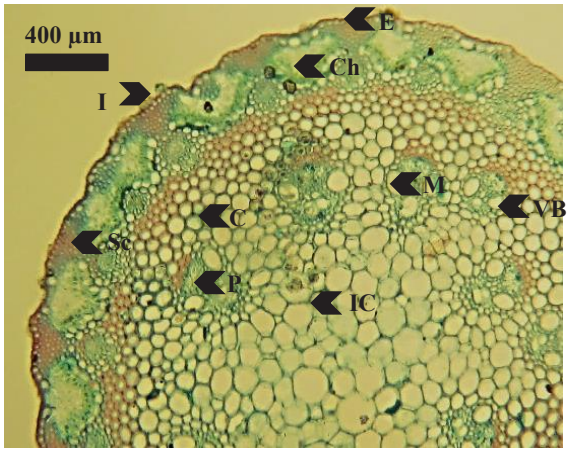

[a) NW] C: Small circular outer cortical cells, **Ch:** Small chlorenchyma cells for performing photosynthesis via stem **E:** Intensive sclerification in epidermis, **I:** highly inveginatedd stem to break wind velocity, , **IC:** Largest cells in inner cortex with 30% area coverd by VB, **M:** Large metaxylem vessels, **Sc:** Intensive sclerification arround vascular bundles and in outer cortical region **VB:** Large vascular bundles

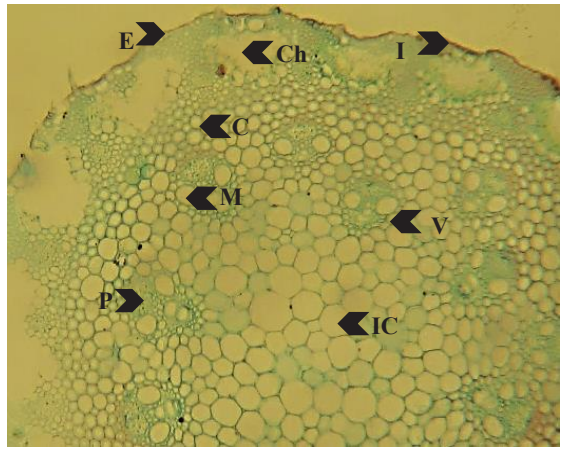

[b) KK] C: Small oval shaped compactly arranged outer cortical cells, **Ch:** Large chlorenchyma cells for performing photosynthesis via stem **E:** Small epidermal cells with intensive sclerification outside, **I:** Moderately inveginatedd stem to break wind velocity, **IC:** Largest cells in inner cortex with 20% area coverd by VB, **M:** Relatively small metaxylem vessels, **Sc:** Intensive sclerification arround vascular bundles and in outer cortical region **VB:** Medium sized vascular bundles

c) NT] C: Small outer cortical cells, **Ch:** Medium sized chlorenchyma cells for performing photosynthesis via stem **E:** Large epidermal cells with intensive sclerification outside, **IC:** Medium sized cells in inner cortex, **M:** Relatively small metaxylem vessels, **Sc:** Slight sclerification arround vascular bundles and in outer cortical region **VB:** Small sized vascular bundles

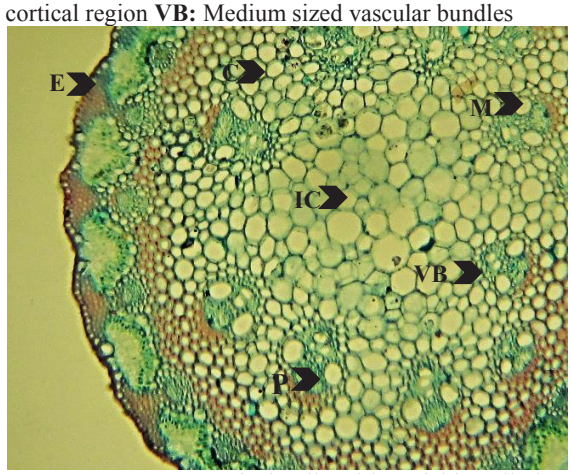

[d) CH] C: Outer cortical cells with variable cell size, **Ch:** Small chlorenchyma cells for performing photosynthesis via stem **E:** Small epidermal cells with intensive sclerification outside, **IC:** Smallest cells in inner cortex, **M:** Relatively small metaxylem vessels, **Sc:** Intensive sclerification arround vascular bundles and in outer cortical region **VB:** Small sized vascular bundles

Figure 12. Stem transverse sections of *Stipagrostis plumosa* L. collected from different sites in the Punjab. All figures are captured at same resolution (40X). Scale bar is given in Figure 12a. Sites abbreviations: NeW: Neela Wahn; KKr: Kallar Kahar; NpT: Noorpur Thal; Cho: Cholista

layers are able to resist soil compaction and cortex is vital for the storage of water under water deficit conditions. Sclerification in the outer cortical region and epidermis protects delicate cortical issue from collapse (Quintana-Pulido et al., 2018). There was a drastic change in root epidermal thickness, epidermal cell area, the proportion of cortical parenchyma, metaxylem area, and phloem area, all of which reduced significantly at the highest water deficit area such as Cho and NpT populations. These adaptations may contribute significantly to species' existence by providing mechanical strength to root tissue and hence preventing soft tissues from collapsing in addition to minimizing water loss during water deficit areas (Zhu et al., 2021). Plants growing at NpT and Cho sites showed

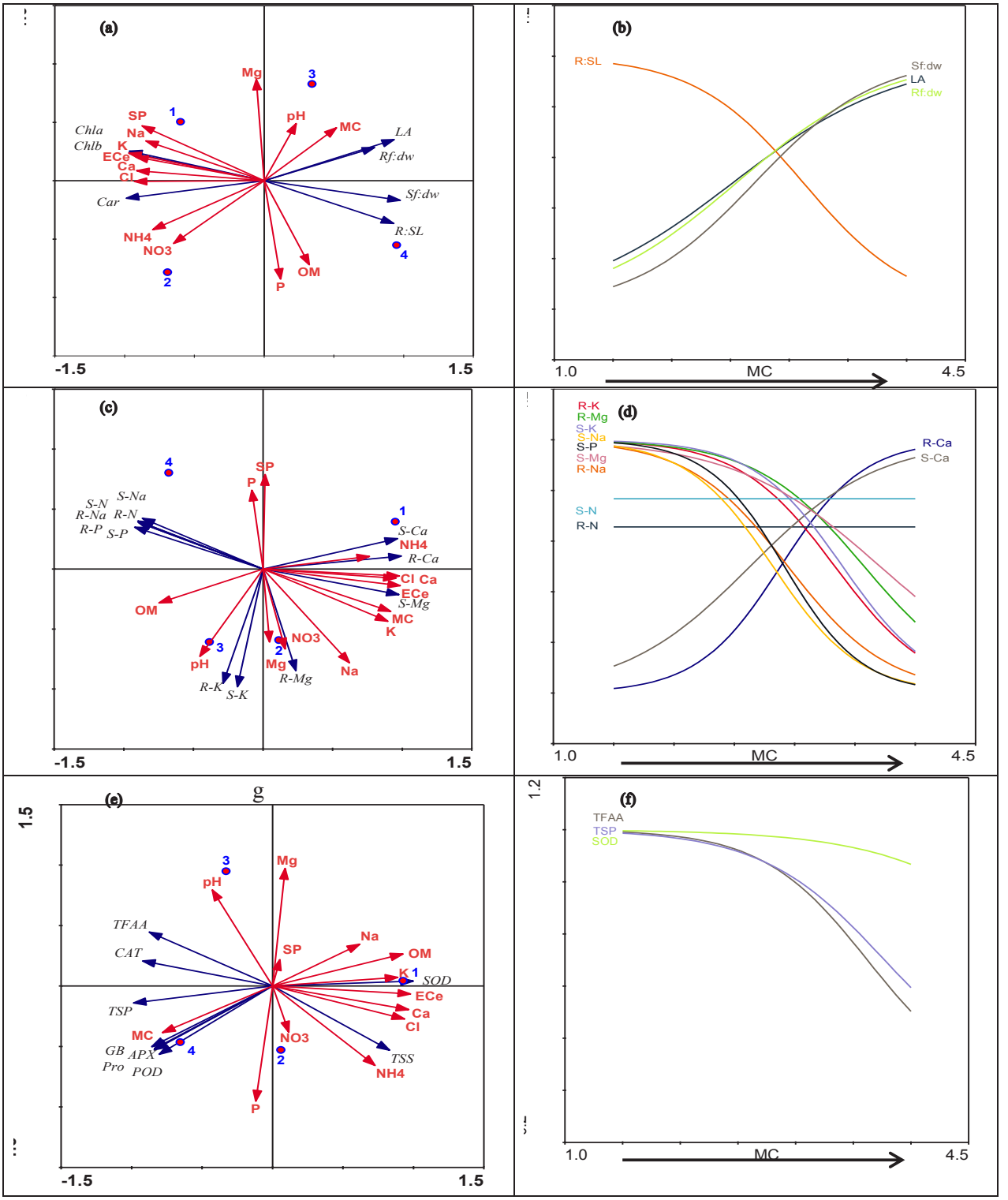

Figure 13. RDA tri-plot and response curves for morpho-physiological (a, b), ionic content (c, d) and antioxidants (e, f) plotted against physico-chemical attributes of *S. plumosus* rhizospheric soil collected from various arid habitats. Response curves were generated against increasing soil moisture from 1% to 4.5% from left to right (as shown by direction of the arrow). Site abbreviations 1 = NeW; 2 = KKr; 3 = NpT; 4 = Cho

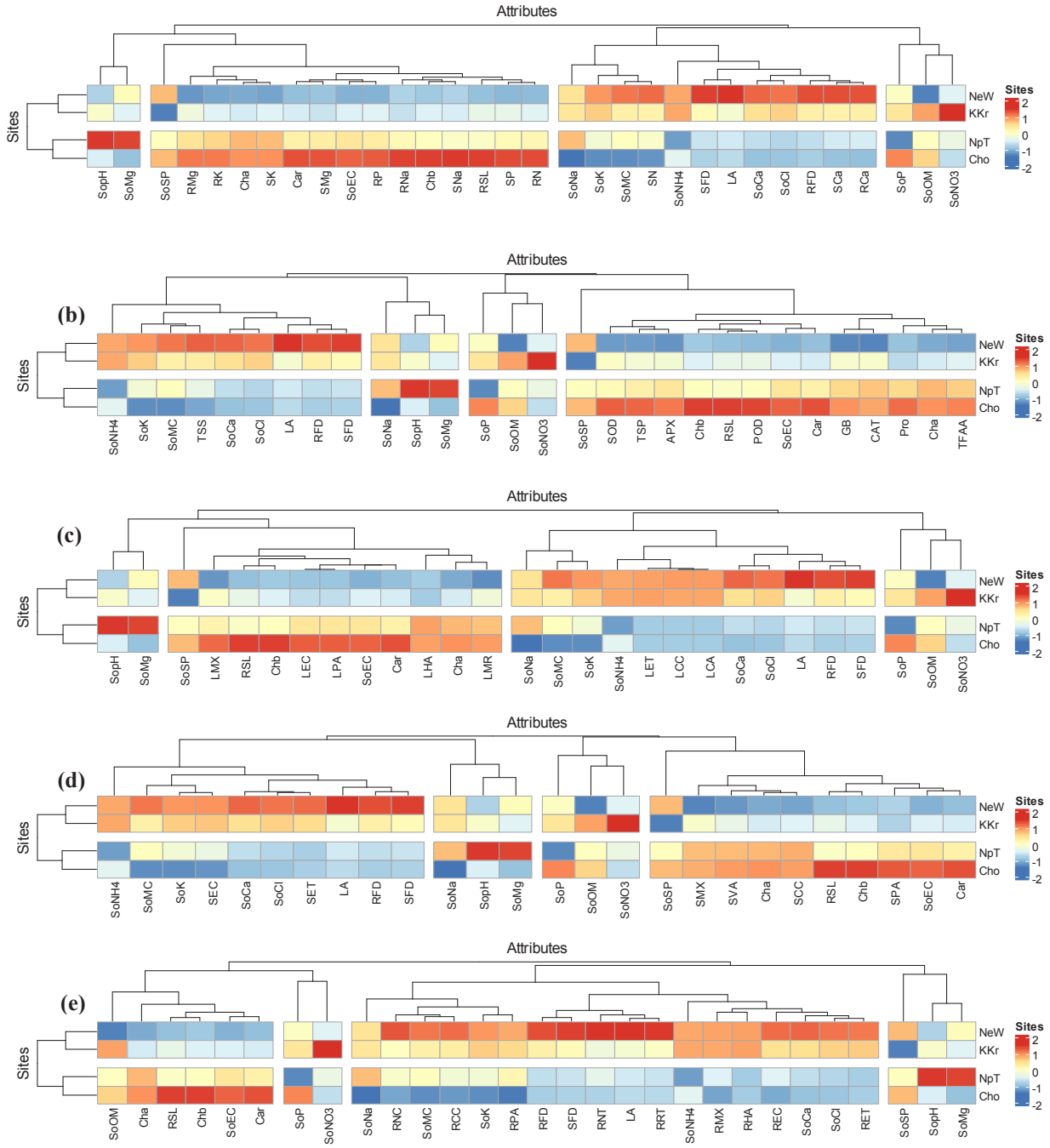

Figure 14. A heatmap showing the influence of soil physico-chemical properties on root and shoot ionic contents (a), biochemical attributes and activities of antioxidative enzymes (b), leaf anatomical attributes (c), shoot anatomical attributes (d) and root anatomical attributes (e) contributing towards growth sustainability of *Stipagrostis plumosa* L. in hyperarid environments. Abbreviations are given at start of the manuscript.

increased sclerification of stem epidermis and increased cortical region, metaxylem and phloem cell areas under soil moisture deficit. Sclerification is extremely beneficial, preventing inner metabolically active tissue from freezing and desiccation (Ahmad et al., 2016; Bi et al., 2017).

In arid zone grasses like *S. plumosa* leaf blade is protected by thickness in epidermis and cortical region (Pescador et al., 2015). Large cortical parenchyma in the leaf enhances the ability to store water when water is a vital entity. This type of succulence has already been

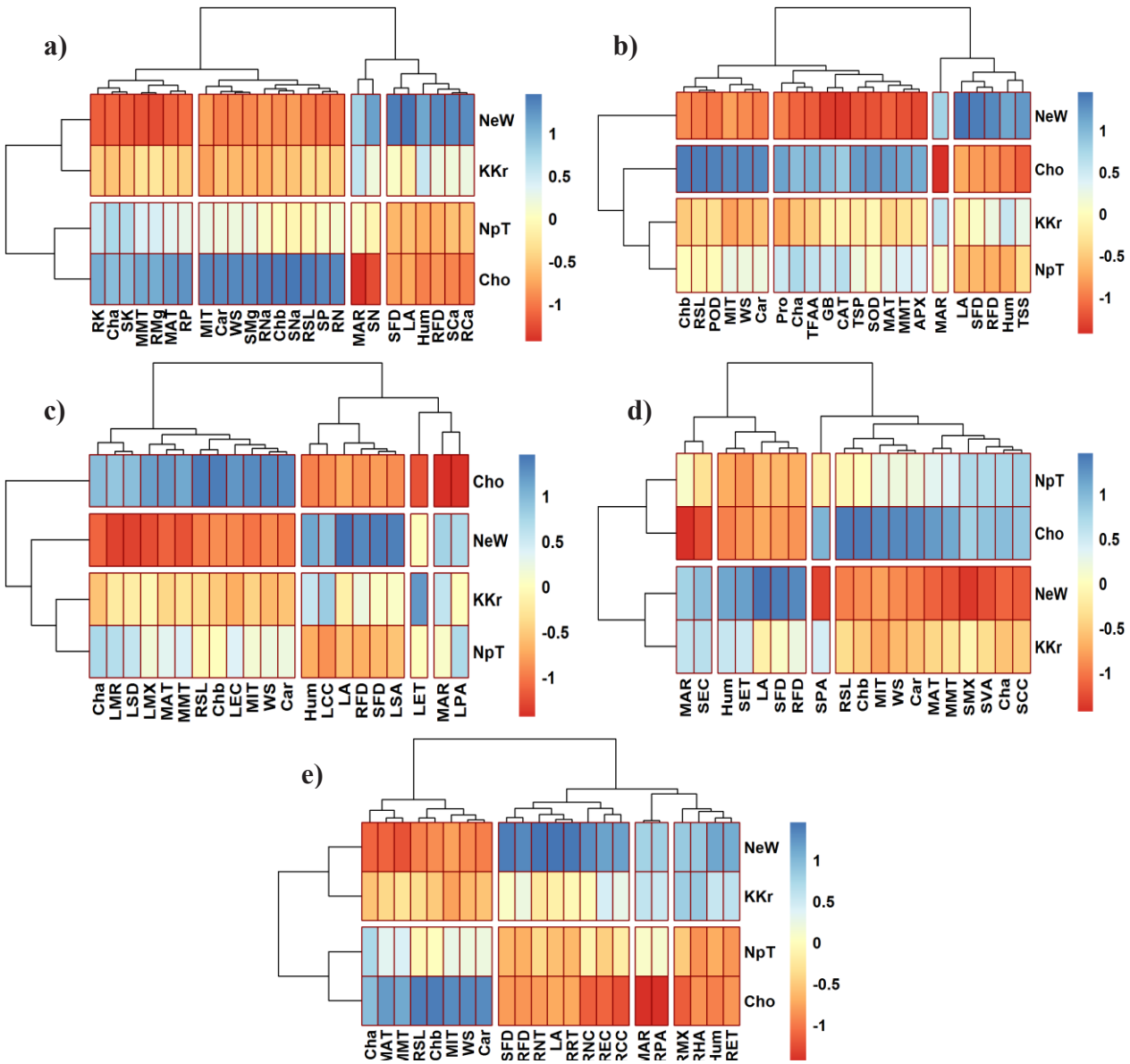

Figure 15. A heatmap showing the influence of climatic variables on root and shoot ionic contents (a), biochemical attributes and activities of antioxidative enzymes (b), leaf anatomical attributes (c), shoot anatomical attributes (d) and root anatomical attributes (e) contributing towards growth sustainability of *Stipagrostis plumosa* L. in hyperarid environments. Abbreviations are given at start of the manuscript.

reported in grasses (Brule et al., 2016; Rayner et al., 2016). Sclerification was recorded in vascular bundles hence making leaves more fibrous and stiff (Bellasio and Lundgren, 2016; Riboldi et al., 2016). Metaxylem vessels were the widest in plants from NpT and Cho followed by NeW and KKr populations. Transpirational losses can be managed by anatomical modifications like thick epidermis, cuticle and long dense hairs. Long hairs on the leaf surface control temperature by developing moisture layer between leaf surface and outside environment (Konrad et al., 2015). Plants growing in NpT and NeW sites had large trichomes that densely covered leaf surface. Stomatal density and area on abaxial leaf surface increased along increasing soil dryness ratio i.e. in NpT and Cho populations. Decreased stomatal density and area in water deficit is the crucial for the regulation of transpiration rate. Small stomata controls transpiration rate more effectively and thus protects plants from water stress (Grubb et al., 2015).

Rainfall on a larger time scale in arid region is probably reflected by the soil moisture content. The anatomical attributes including sclerification and thicker epidermis, well-developed water-storing tissues can have a direct

link to the rainfall patterns (Naz et al. 2013). Presently, clustered heatmap showed that humidity (Hum) in general was linked to mean annual rainfall (MAR) and temperatures (MAT, MMT, and MIT) that strongly affected many growth, physiological, and, stem, root and leaf anatomical attributes. This suggests that *S. plumosa* plants ensured survival by modifying according to changing environmental conditions particularly under water deficit conditions (Peel et al. 2017).

5. Conclusion

It was concluded that phenotypic plasticity (both structural and functional modifications) in *S. plumosa* enabled it to survive in arid environments. The features shared by NeW and KKr populations included large root cortical cells with intensive sclerification around vascular bundles to store additional water and avoid tissue collapse, large chlorenchyma cells for performing photosynthesis via stem, highly invaginated stem and leaf surface to break wind velocity and leaf rolling. The NpT and Cho populations showed longer roots for absorption of water from deeper layers of soil and stunted growth as metabolic energy was involved in survival than normal vegetative growth. These populations exhibited smaller leaf areas to reduce transpiration rates by reducing light interception and more carotenoids content to scavenge singlet oxygen species for the protection of their photosynthetic apparatus. Higher accumulation of osmolytes leads to decreased osmotic potential and modulated plant water potential for enhancing water uptake in extremely moisture deficit conditions. Dendrite-shaped leaf epidermal cell's invagination was a key feature to increase the cell surface area for controlling water flux in epidermal cells. On the basis of Generalized Linear Model (GLM), all observed attributes were divided into three groups, nonplastic, positively plastic and negatively plastic. Shoot ions (S-N), root ions (R-N, R-P), organic osmolytes (TSS, GB, Pro) and antioxidants (APX, POD, CAT) showed a nonplastic response. Plastic traits (positively sloped) growth (R:SL), shoot ions (P, Mg, K, Na), root ions (Mg, K, Na), osmolytes (TFAA, TSP) and antioxidants (SOD). Negatively sloped plastic traits were growth (Rf:dwt, leaf area), root ions (RCa) and shoot ions (SCa).

List of Abbreviations:

Climatic Variables: MAR, Mean annual rainfall; MAT, Mean annual temperature; MMT, Maximum annual temperature; MIT, Minimum annual temperature; Hum, Humidity; WS, Wind speed

Sites abbreviations: NeW, Neela Wahn; KKr, Kallar Kahar; NpT, Noorpur Thal; Cho, Cholistan

Soil attributes: SoMC, Soil moisture contents; SopH, Soil pH; SoEC, Soil EC; SoNa, Soil sodium; SoK, Soil potassium; SoCa, Soil calcium; SoMg, Soil magnesium; SoCl, Soil chloride, SoP, Soil phosphate (PO_4^{3-}), SoOM, Soil organic matter, $SoNH_4$, Soil ammonium, $SoNO_3$; Soil nitrate

Plant attributes: R: SL, Root to shoot length; S f: d wt. Shoot fresh to dry weight ratio; R f: d wt. Root fresh to dry weight ratio; LA, Leaf area; SOD, Superoxide dismutase; APX, Ascorbate peroxidase; POD, Peroxidase; CAT, Catalase; TSS, Total soluble sugars; TSP, Total soluble proteins; GB, Glycinebetaine; Pro, Proline; TFAA, Total free amino acids

Root anatomy: RET, Root epidermal thickness; RRT, Root cortical region thickness; RNT, Root endodermal thickness; RMX, Root metaxylem area; RPA, Root pith area; REC, Root epidermal cell area; RCC, Root cortical cell area; RNC, Root endodermal cell area; RHA, Root phloem area

Stem Anatomy: SPA, Stem pith area; SET, Stem epidermal thickness; SCC, Stem cortical cell area; SMX, Stem metaxylem area; SEC, Stem epidermal cell area; SVA, Stem vascular bundle area

Leaf anatomy: LMR, Leaf midrib thickness; LEC, Leaf epidermal cell area; LMX, Leaf metaxylem area; LPA, Leaf phloem area; LET, Leaf epidermal thickness; LCC, Leaf cortical cell area; LSD, Leaf stomatal density; LSA, Leaf stomatal area

References

Adnan S, Ullah K, Khan AH, Gao S (2017). Meteorological impacts on evapotranspiration in different climatic zones of Pakistan. Journal of Arid Land 9 (6): 938–52. doi: 10.1007/s40333-017-0107-2

Ahmad KS, Hameed M, Deng J, Ashraf M, Hamid A et al. (2016). Ecotypic adaptations in Bermuda grass (*Cynodon dactylon*) for altitudinal stress tolerance. Biologia 71: 885–895. doi: 10.1515/biolog-2016-0113

Arif Y, Singh P, Siddiqui H, Bajguz A, Hayat S (2020). Salinity induced physiological and biochemical changes in plants: an omic approach towards salt stress tolerance. Plant Physiology and Biochemistry 156: 64–77. doi: 10.1016/j.plaphy.2020.08.042

Arnon DI (1949). Copper enzymes in isolated chloroplasts. Polyphenoloxidase in *Beta vulgaris*. Plant Physiology 24 (1):1–15. doi: 10.1104/pp.24.1.1

Bahar NH, Hayes L, Scafaro AP, Atkin OK, Evans JR (2018). Mesophyll conductance does not contribute to greater photosynthetic rate per unit nitrogen in temperate compared with tropical evergreen wet-forest tree leaves. New Phytologist 218: 492–505. doi: 10.1111/nph.15031

Bates LS, Waldren RP, Teare I (1973). Rapid determination of free proline for waterstress studies. Plant and Soil 39 (1): 205–207. doi: 10.1007/BF000180

Bellasio C, Lundgren MR (2016). Anatomical constraints to C_4 evolution: light harvesting capacity in the bundle sheath. New Phytologist 212: 485–496. doi: 10.1111/nph.14063

Bi HH, Kovalchuk N, Langridge P, Tricker PJ, Lopato S et al. (2017). The impact of drought on wheat leaf cuticle properties BMC Plant Biology 17: p. 85. doi: 10.1186/s12860-017-1033-3

Bradford MM (1976). A rapid and sensitive method for the quantitation of microgram quantities of protein utilizing the principle of protein-dye binding. Analytical Biochemistry 72 (1–2): 248–54. doi: 10.1016/0003-2697(76)90527-3

Brule V, Rafsanjani A, Pasini D, Western TL (2016). Hierarchies of plant stiffness. Plant Science 250: 79–96. doi: 10.1016/j.plantsci.2016.06.002

Budyko MI (1958) The Heat Balance of the Earth's Surface. Soviet Geography, 2:4, 3-13, doi: 10.1080/00385417.1961.10770761

Chance B, Maehly A (1955). Assay of catalases and peroxidases. Methods of Biochemical Analysis 1: 357–424. doi: 10.1002/9780470110171.ch14

Chavoshi S, Nourmohamadi G, Hamid M, Abad HHS, Fazel MA (2018). The effects of biofertilizers on physiological traits and biomass accumulation of red beans (*Phaseolus vulgaris* cv. Goli) under water stress. Iranian Journal of Plant Physiology 8: 2555–2562. doi: 10.22034/ijpp.2018.543427

Cuizhi F, Xinyi W, Xin G, Chunfang Z, Haiyan Z et al. (2021). Concentration effects and its physiological mechanism of soaking seeds with brassinolide on tomato seed germination under salt stress. Acta Ecologica Sinica 41: 1857–1867. doi: 10.3390/su13115976

Davis D, Armond P, Gross E, Arntzen CJ (1976). Differentiation of chloroplast lamellae onset of cation regulation of excitation energy distribution. Archives of Biochemistry and Biophysics 175 (1): 64–70. doi: 10.1016/0003-9861(76)90485-9

Dhief A, Aschi-Smiti S, Neffati M (2022). Floristic diversity and plant composition of the arid and Saharan zones of southern Tunisia. GSC Biological and Pharmaceutical Sciences, 18 (03): 250–273. doi: 10.30574/gscbps.2022.18.3.0081

Dixit P, Ghaskadbi S, Mohan H, Devasagayam TP (2002). Antioxidant properties of germinated fenugreek seeds. Phytotherapy Research 19 (11): 977–983. doi: 10.1002/ptr.1769

Eziz A, Yan Z, Tian D, Han W, Tang Z et al. (2017). Drought effect on plant biomass allocation: A meta-analysis. Ecology and Evolution 7: 11002–11010. doi: 10.1002/ece3.3630

Gavlak R, Horneck D, Miller D (2005). Plant, soil and water reference methods for the Western Region. Western Regional Extension Publication (WREP) 125, WERA-103 Technical Committee.

Giannopolitis CN, Ries SK (1977). Superoxide dismutases: I. Occurrence in higher plants. Plant Physiology 59 (2): 309–314. doi: 10.1104/pp.59.2.309

Grieve CM, Grattan SR (1983). Rapid assay for determination of water-soluble quaternary amino compounds. Plant and Soil 70 (2): 303–307. doi: 10.1007/BF02374789

Grubb PJ, Maranon T, Pugnaire FI, Sack L (2015). Relationships between specific leaf area and leaf composition in succulent and non-succulent species of contrasting semi-desert communities in south-eastern Spain. Journal of Arid Environment 118: 69–83. doi: 10.1016/j.jaridenv.2015.03.001

Hamilton P, Van-lyke D (1973). Amino acid determination with ninhydrin. Journal of Biological Chemistry 150 (1): 231–50. doi: 10.1016/S0021-9258(18)51268-0

Hare FK (2019). Energy-based climatology and its frontier with ecology. In Directions in geography, 171–92. London: Routledge. Ebook ISBN 9780429273292

Hare RD (1985). Comparison of procedures for the assessment of psychopathy. Journal of Consulting and Clinical Psychology 53 (1): 7–16. doi: 10.1037/0022-006X.53.1.7

Huang J, Ji M, Xie Y, Wang S, He Y et al. (2016). Global semi-arid climate change over last 60 years. Climate Dynamics 46 (3): 1131-1150. doi: 10.1007/s00382-015-2636-8

Ivanova LA, Yudina PK, Ronzhina DA, Ivanov LA, Holzel N (2018). Quantitative mesophyll parameters rather than whole-leaf traits predict response of C3 steppe plants to aridity. New Phytologist 2017: 558–570. doi: 10.1111/nph.14840

Jan M, Anwar-ul-Haq M, Adnan NS, Muhammad Y, Javaid I et al. (2019). Modulation in growth, gas exchange, and antioxidant activities of salt-stressed rice (*Oryza sativa* L.) genotypes by zinc fertilization. Arabian Journal of Geosciences 12: 2-7. doi: 10.1007/s12517-019-4939-2

Kapoor D, Bhardwaj S, Landi M, Sharma A, Ramakrishnan M et al. (2020). The impact of drought in plant metabolism: How to exploit tolerance mechanisms to increase crop production. Applied Sciences 10: 1-19. doi: 10.3390/app10165692

Karimpour T, Safaei E, Karimi B (2019). A supported manganese complex with aminebis(phenol) ligand for catalytic benzylic C(sp3)–H bond oxidation. RSC Advances 9: 14343–14351. doi: 10.1039/c9ra02284h

Kidd D, Ryan M, Colmer TD, Simpson R (2021). Root growth response of *Serradella* species to aluminium in solution culture and soil. Grass and Forage Science 76 (1): 57–71. doi: 10.1111/gfs.12528

Kidd D, Ryan M, Hahne D, Haling RE (2018). The carboxylate composition of rhizosheath and root exudates from twelve species of grassland and crop legumes with special reference to the occurrence of citra malate. Plant and Soil 424: 1–2. doi: 10.1007/s11104-017-3534-0

Kidron GJ (2019). The dual effect of sand-covered biocrusts on annual plants: increasing cover but reducing individual plant biomass and fecundity. Catena 182: 104120. doi: 10.1016/j.catena.2019.104120

Konrad W, Burkhardt J, Ebner M, Roth-Nebelsick A (2015). Leaf pubescence as a possibility to increase water use effciency by promoting condensation. Ecohydrology 8: 480–492. doi: 10.1002/eco.1518

Kowalenko C, Lowe L (1973). Determination of nitrates in soil extracts. Soil Science Society of America Journal, 37: 660–660. doi: 10.2136/sssaj1973.03615995003700040051x

Lettau H (1969). Evapotranspiration climatonomy: I. A new approach to numerical prediction of monthly evapotranspiration, runoff, and soil moisture storage. Monthly Weather Review 97 (10): 691–699. doi: 10.1175/1520-0493

Lopes DM, Walford N, Viana H, Junior CRS (2016). A proposed methodology for the correction of the leaf area index measured with a ceptometer for *Pinus* and *Eucalyptus* forests. Revista Arvore, Brazilian Journal of Forest Science 40: 845–854. doi: 10.1590/0100-67622016000500008

Louhaichi M, Gamoun M, Hassan S, Abdallah MAB (2021). Characterizing Biomass Yield and Nutritional Value of Selected Indigenous Range Species from Arid Tunisia. Plants 10: 1–18. doi: 10.3390/plants10102031

Majeed M, Tariq A, Haq SM, Waheed M, Anwar MM et al. (2022). A detailed ecological exploration of the distribution patterns of wild poaceae from the Jhelum District (Punjab), Pakistan. Sustainability, 14: 1–17. doi: 10.3390/su14073786

Masouleh SS, Aldine NJ, Sassine YN (2019). The role of organic solutes in the osmotic adjustment of chilling-stressed plants (vegetable, ornamental and crop plants). Ornamental Horticulture, 25: 434–442. doi: 10.1590/2447-536x.v25i4.2073

Morris H, Plavcova L, Goral M, Klepsch MM, Kotowska M et al. (2018). Vessel-associated cells in angiosperm xylem: Highly specialized living cells at the symplast-apoplast boundary. American Journal of Botany 105: 1–10. doi: 10.1002/ajb2.1030

Nakano Y, Asada K (1981). Hydrogen peroxide is scavenged by ascorbate-specific peroxidase in spinach chloroplasts. Plant and Cell Physiology 22: 867–80. doi: 10.1093/oxfordjournals.pcp.a076232

Naz N, Hameed M, Nawaz T, Batool R, Ashraf M et al (2013). Structural adaptations in the desert halophyte Aeluropus lagopoides (Linn.) Trin. ex Thw. under high salinity. Journal of Biological Research, 19, 150–164

Nathan KKr, Sinha SK (1996) Moisture Deficit Index Evaluated for Dry Regions of India. Drought Network News (1994-2001). 60. University of Nebraska – Lincoln, Nebraska, USA.

Pescador DS, de-Bello F, Valladares F, Escudero A (2015). Plant trait variation along an altitudinal gradient in Mediterranean high mountain grasslands: controlling the species turnover. PLoS One 10, e0118876. doi: 10.1371/journal.pone.0118876

Peel JR, Sánchez MCM, Portillo JL, Golubov, J (2017). Stomatal density, leaf area and plant size variation of *Rhizophora mangle* (Malpighiales: Rhizophoraceae) along a salinity gradient in the Mexican Caribbean. Revista de Biología Tropical 65 (2): 701–712. doi: 10.15517/rbt.v65i2.24372

Quintana-Pulido C, Villalobos-González L, Munoz M, Franck N, Pastenes C (2018). Xylem structure and function in three grapevine varieties. Chilean Journal of Agricultural Research 78: 419–428. doi: 10.4067/s0718-58392018000300419

Rayner JP, Farrell C, Raynor KJ, Murphy SM, Williams NS (2016). Plant establishment on a green roof under extreme hot and dry conditions: the importance of leaf succulence in plant selection. Urban Forestry and Urban Greening 15: 6–14. doi: 10.1016/j.ufug.2015.11.004

Riboldi LB, Oliveira RF, Angelocci LR (2016). Leaf turgor pressure in maize plants under water stress. Australian Journal of Crop Science 10: 878. doi: 10.21475/ajcs.2016.10.06.p7602

Rose R, Rose CL, Omi SK, Forry KR, Durall DM et al. (1991). Starch determination by perchloric acid vs enzymes: evaluating the accuracy and precision of six colorimetric methods. Journal of Agricultural and Food Chemistry 39: 2-11. doi: 10.1021/jf00001a001

Ruzin SE (1999). Plant microtechnique and microscopy. New York, NY: Oxford University Press. ISBN-10: 0195089561

Sparks DL (1996) Methods of Soil Analysis Part 3: Chemical Methods. Soil Science Society of America, American Society of Agronomy, Madison. ISBN: 978-0-891-18825-4

Sun M, Chen HH, Xu JP, Yue HT, Tian K (2018). Evolutionary associations of leaf functional traits in nine Euphorbiaceae species. International Journal of Agriculture and Biology 20: 1309–1317. doi: 10.17957/IJAB/15.0631

Susetyarini E, Wahyono P, Latifa R, Nurrohman E (2020). The Identification of Morphological and Anatomical Structures of *Pluchea indica*. Journal of Physics 1539: 1–13. doi: 10.1088/1742-6596/1539/1/012001

Ter Braak TCJF, Smilauer P (2002) CANOCO reference manual and CanoDraw for Windows user's guide: Software for Canonical Community Ordination (version 4.5). Biometris, Wageningen. doi: 10.1017/CBO9781139627061

Thapa S, Rudd JC, Xue QW, Bhandari M, Reddy SK et al. (2019). Use of NDVI for characterizing winter wheat response to water stress in a semi arid environment. Journal of Crop Improvement, 33: 633-648. doi: 10.1080/15427528.2019.1648348

UNEP (1997). World Atlas of Desertification. London, UK.

UNESCO (1979). Map of the World Distribution of Arid Regions, MAB Technical Note 7. Paris: UNESCO.

Walkley A (1947). A critical examination of a rapid method for determining organic carbon in soils—effect of variations in digestion conditions and of inorganic soil constituents. Soil Science 63: 251–264. doi: 10.1097/00010694-194704000-00001

Wellband KW, Heath DD (2017). Plasticity in gene transcription explains the differential performance of two invasive fish species. Evolutionary Applications, 10 (6): 563–576. doi: 10.1111/eva.12463

Verheye W (1976). Nature and Impact of Temperature and Moisture in Arid Weathering and Soil Forming Processes - A Review. Pedologie, 26 (3): 205-224.

Wolf B (1982). A comprehensive system of leaf analyses and its use for diagnosing crop nutrient status. Communications in Soil Science and Plant Analysis 13 (12): 1035–1059. doi: 10.1080/00103628209367332

Yang Y, Anderson MC, Gao F, Wardlow B, Hainc CR et al. (2018). Field-scale mapping of evaporative stress indicators of crop yield: An application over Mead, NE, USA. Remote Sensing of Environment 210: 387–402. doi: 10.1016/j.rse.2018.02.020

Yoshida S, Forno DA, Cock JH (1971). Laboratory manual for physiological studies of rice. The International Rice Research Institute, Philippines, Los Baños, Philippines.

Zahoor A, Ahmad F, Hameed M, Basra SMA (2018). Contribution of structural and functional traits in turgor maintenance of *Pistia stratiotes* under cadmium toxicity. International Journal of Agriculture and Biology 20: 1391–1396. doi: 10.17957/IJAB/15.0647

Zhou L, Tian X, Cui B, Hussain A (2021). Physiological and biochemical responses of invasive species *Cenchrus pauciflorus* benth to drought stress. Sustainability 13: 59–76. doi: 10.3390/su13115976

Zhu J, Cai D, Wang J, Cao J, Wen Y et al. (2021). Physiological and anatomical changes in two rapeseed (*Brassica napus* L.) genotypes under drought stress conditions. Oil Crop Science 6: 97–104. doi: 10.1016/j.ocsci.2021.04.003

Zhuang WW, Serpe M, Zhang YM (2015). The effect of lichen-dominated biological soil crusts on growth and physiological characteristics of three plant species in a temperate desert of northwest China. Plant Biology 17 (6): 1165–1175. doi: 10.1111/plb.12359